

# Physics of neutralization of intense high-energy ion beam pulses by electrons<sup>a)</sup>

I. D. Kaganovich,<sup>1,b)</sup> R. C. Davidson,<sup>1</sup> M. A. Dorf,<sup>1</sup> E. A. Startsev,<sup>1</sup> A. B. Sefkow,<sup>1,c)</sup>  
E. P. Lee,<sup>2</sup> and A. Friedman<sup>3</sup>

<sup>1</sup>Princeton Plasma Physics Laboratory, Princeton, New Jersey 08543, USA

<sup>2</sup>Lawrence Berkeley National Laboratory, Berkeley, California 94720, USA

<sup>3</sup>Lawrence Livermore National Laboratory, Livermore, California 94550, USA

(Received 25 November 2009; accepted 5 February 2010; published online 23 March 2010)

Neutralization and focusing of intense charged particle beam pulses by electrons form the basis for a wide range of applications to high energy accelerators and colliders, heavy ion fusion, and astrophysics. For example, for ballistic propagation of intense ion beam pulses, background plasma can be used to effectively neutralize the beam charge and current, so that the self-electric and self-magnetic fields do not affect the ballistic propagation of the beam. From the practical perspective of designing advanced plasma sources for beam neutralization, a robust theory should be able to predict the self-electric and self-magnetic fields during beam propagation through the background plasma. The major scaling relations for the self-electric and self-magnetic fields of intense ion charge bunches propagating through background plasma have been determined taking into account the effects of transients during beam entry into the plasma, the excitation of collective plasma waves, the effects of gas ionization, finite electron temperature, and applied solenoidal and dipole magnetic fields. Accounting for plasma production by gas ionization yields a larger self-magnetic field of the ion beam compared to the case without ionization, and a wake of current density and self-magnetic field perturbations is generated behind the beam pulse. A solenoidal magnetic field can be applied for controlling the beam propagation. Making use of theoretical models and advanced numerical simulations, it is shown that even a small applied magnetic field of about 100 G can strongly affect the beam neutralization. It has also been demonstrated that in the presence of an applied magnetic field the ion beam pulse can excite large-amplitude whistler waves, thereby producing a complex structure of self-electric and self-magnetic fields. The presence of an applied solenoidal magnetic field may also cause a strong enhancement of the radial self-electric field of the beam pulse propagating through the background plasma. If controlled, this physical effect can be used for optimized beam transport over long distances. © 2010 American Institute of Physics. [doi:10.1063/1.3335766]

## I. INTRODUCTION

Neutralization and focusing of intense charge particle beams by background plasma form the basis for a variety of applications to high-energy accelerators and colliders,<sup>1-3</sup> astrophysics,<sup>4-7</sup> inertial confinement fusion, in particular, fast ignition<sup>8</sup> and heavy ion fusion,<sup>9-12</sup> magnetic fusion based on field-reversed configurations fueled by energetic ion beams,<sup>13</sup> the physics of solar flares,<sup>14</sup> high-intensity high-energy particle beam propagation in the atmosphere and outer-space plasmas,<sup>15</sup> as well as basic plasma physics phenomena.<sup>16</sup> For instance, one of the modern approaches to ion beam compression for heavy ion fusion applications is to use a dense background plasma, which charge neutralizes the ion charge bunch, and hence facilitates compression of the charge bunch against strong space-charge forces.<sup>9,10,17-20</sup>

For heavy ion fusion applications, the space-charge potential of the ion beam pulse is of order 100 V at the exit of the accelerator and can reach 10 kV at the end of compression phase.<sup>9,10</sup>

The potential energy of the space-charge potential is much greater than the temperature of the beam ions, which is set by the ion source emitter and is of order 0.1 eV.<sup>9,10</sup> Therefore, ion beams used for heavy ion fusion applications are space-charge (perveance) dominated, i.e., the space-charge potential energy is large compared with the ion beam temperature, or equivalently, the perveance term in the equation for the beam envelope is large compared with the emittance term.<sup>11,12</sup> For example, for the Neutralized Drift Compression eXperiment-I (NDCX-I),<sup>9,10</sup> the perveance  $Q = 2\pi e^2 Z_b^2 n_b r_b^2 / \gamma_b^3 M V_b^2 \sim 10^{-3}$ , and the emittance is  $\varepsilon \sim 30\pi$  mm mrad; the beam radius in the extraction region of the ion beam source is 2.5 cm and can be reduced using an aperture. The evolution of the beam radius,  $r_b$ , can be assessed by making use of the beam envelope equations,<sup>9,10</sup>

$$\frac{d^2 r_b}{dz^2} = \frac{Q}{r_b} + \frac{\varepsilon^2}{r_b^3}. \quad (1)$$

From Eq. (1), it is evident for NDCX-I experimental parameters that the perveance term (the first term on the right-hand side) dominates the emittance term (the second term on the right-hand side). For perveance-dominated beams, one can

<sup>a)</sup>Paper CI2 2, Bull. Am. Phys. Soc. 54, 54 (2009).

<sup>b)</sup>Invited speaker.

<sup>c)</sup>Current address at Sandia National Laboratories, Albuquerque, NM 87185.

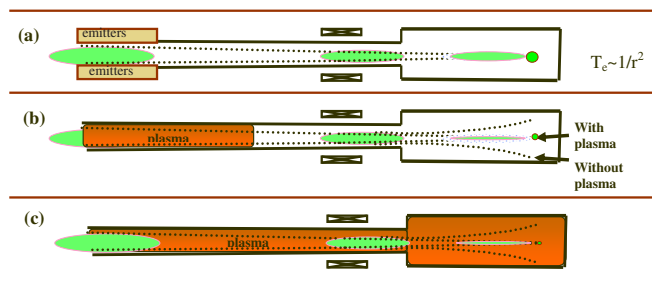


FIG. 1. (Color online) Schematics of different neutralization methods.

readily integrate Eq. (1) neglecting the emittance term and obtain

$$(dr_b/dz)^2 = r_i'^2 + 2Q \ln(r_b/r_i), \quad (2)$$

where  $r_i' = dr_b/dz|_i$  is the initial angle of beam convergence. For example, from Eq. (2), it can be shown that if the beam ballistically propagates without an initial convergence angle ( $r_i' = 0$ ) or an applied focusing field or neutralization, the beam radius increases from an initial radius  $r_i$  to a twice larger radius  $2r_i$  after propagating a distance

$$\int_{r_i}^{2r_i} dr/\sqrt{2Q \ln(r/r_i)} \approx 1.5r_i/\sqrt{Q}. \quad (3)$$

For typical NDCX-I parameters,<sup>9,10</sup> this distance is of order 1 m and is shorter than the length of the drift section. Therefore, the beam space charge has to be effectively neutralized during ballistic drift. For future heavy ion fusion drivers with energy and current larger than the NDCX-I parameters<sup>9</sup> the perveance remains of order  $Q \sim 10^{-3}$  and the drift sections are longer than a meter.<sup>18–22</sup> Therefore the beam space charge has to be effectively neutralized for all future HIF facilities. Besides neutralized drift compression, the ion beam pulses need to be radially compressed. For heavy ion fusion applications, the beam pulse is focused over distances of 1–5 m, corresponding to the reactor chamber size;<sup>21,22</sup> during focusing, an initial beam radius of 1–2 cm is reduced to a spot radius of about 1 mm or less (see Fig. 1). For this weak ballistic focusing, the beam space charge has to be neutralized well enough so that the beam convergence angle is not affected by the self-fields of the beam pulse during the drift, i.e., from Eq. (2) it follows that the degree of charge neutralization,  $f$ , should satisfy the following condition:

$$2(1-f)Q \ln(r_i/r_f) \ll r_i'^2. \quad (4)$$

Substituting the estimates  $r_i' \sim 10^{-2}$ ,  $Q \sim 10^{-3}$ , and  $r_i/r_f \sim 10$  into Eq. (4), we obtain that the degree of neutralization should be better than  $(1-f) \ll 10^{-2}$ , or *better than 99%*. That is, for a heavy ion fusion driver, the beam self-field potential is initially of order 10 kV, whereas the self-field potential after neutralization should be less than 100 V.

Numerical studies<sup>21,22</sup> have shown that neutralization by background plasma can achieve the required degree of charge neutralization.

This paper presents a survey of the present theoretical understanding of the neutralization of intense ion beams by electron sources and a background plasma. The present discussion is focused on high-energy ion beam pulses with ion beam velocity that is large compared to the electron thermal velocity, i.e.,

$$V_b \gg V_{Te}. \quad (5)$$

The typical temperature of background plasma electrons produced in a discharge is of order 3 eV, and the corresponding electron thermal velocity  $V_{Te} \approx \sqrt{2T_e/m}$  is of order  $10^8$  cm/s; in case of filament emission the electron temperature is of order 0.1 eV. The velocity of a 1 MeV potassium ion is  $2.2 \times 10^8$  cm/s. For a heavy ion fusion driver, the beam energy is envisioned to be higher than 300 MeV. Therefore, the criterion in Eq. (5) is well satisfied for future drivers and moderately well satisfied for current experiments. Due to the fast motion of the beam pulse through the background plasma, a return current is generated in the plasma, in which the electron flow velocity is comparable with the beam velocity. Thus the electron flow velocity in the return current is faster than the thermal electron velocity, and this electron flow determines the self-electric and self-magnetic fields of the beam pulse propagating through the background plasma; and the electron potential energy in the self-electric field of the beam pulse propagating through the background plasma is large compared with the electron temperature. Therefore, the electron pressure terms can be neglected for fast ion beam pulses, in contrast to the limit of slow beams, considered, e.g., in Section 4.3.1 of Ref. 23.

In many applications, an external magnetic field is applied for plasma confinement, or for focusing the ion beam. Therefore, the effects of the applied magnetic field on the degree of charge and current neutralization of an intense ion beam pulse propagating through a background plasma have also been investigated.<sup>24–26</sup> It has been recently demonstrated that even a weak magnetic field (about 100 G) can significantly change the degree of charge and current neutralization of an intense ion beam pulse propagating through a background plasma.

The organization of the paper is as follows. Section II briefly describes different schemes to introduce electrons into a positive ion beam pulse for neutralization. Advantages of volumetric plasma present everywhere along the beam pulse propagation are emphasized. Section III identifies the critical plasma parameters that assure very good charge and current neutralization of the ion beam pulse. Sections IV and V summarize major results on the self-electric and self-magnetic fields generated by an intense ion beam pulse propagating in a background plasma. Sections VI–VIII describe the effects of gas ionization and solenoidal and dipole magnetic fields, respectively, on the self-electric and self-magnetic fields of an ion beam pulse propagating in a background plasma. Conclusions are summarized in Sec. IX.

## II. DIFFERENT SCHEMES TO INTRODUCE ELECTRONS INTO A POSITIVE ION BEAM PULSE FOR NEUTRALIZATION

### A. Neutralization by emitting filaments positioned near the beam sides

A very important application of this research is heavy ion fusion, which utilizes a neutralized drift compression scheme to achieve high brightness beam pulses. An effective way to achieve high current density of an ion beam pulse on a target is to simultaneously compress the beam pulse in both the radial and longitudinal directions. This is accomplished by applying a velocity tilt to the beam pulse, so that the beam tail is accelerated relative to the beam head.<sup>10,17,19,20,27</sup> As a result, the beam line charge density increases during the drift compression, when the beam tail approaches the beam head. Similarly, the beam pulse can be compressed radially by passing the beam pulse through a focusing element, for example, a strong solenoidal magnetic lens. Because the self-electric field of the beam increases rapidly during compression, the beam space charge may prevent tight compression, and thus the space charge has to be effectively neutralized. In Ref. 28, it was shown that, because the electron response time is fast compared with the beam pulse duration, the neutralization process can be considered local for any cross section of the beam pulse. Therefore, in the following we focus only on the neutralization process of beam pulses with constant beam velocity. Experimental details of the drift compression scheme are given in Refs. 10, 17, 19, and 20 whereas a theoretical description of limiting factors of the compression scheme are described in Refs. 20 and 27.

To compensate for a large space-charge potential in the neutralized drift compression section of the accelerator, a sufficiently large number of electrons must be introduced. This can be accomplished by supplying electrons from electron emitters positioned at the peripheral region of the transport section.<sup>29-31</sup> Emitted electrons from the emitters positioned near the side region of the ion beam pulse acquire energies of order the unneutralized beam self-field potential. In a stationary electrostatic field, the electrons are reflected back radially toward the emitter. Therefore, the electron density is distributed over distances larger than the beam radius. Hence, one would expect that the degree of charge neutralization to be of order 50% in such a scheme<sup>31,32</sup> (see also Sec. 3.6.2 of Ref. 23). Figures 2 and 3 show the results of simulations making use of the LSP particle-in-cell code.<sup>33</sup> Initially, when the beam pulse is far from the emitting side-walls, the neutralization is poor, of order 50%, as predicted by analytical estimates. As soon as the expanding beam comes in contact with the emitting walls, the neutralization is greatly improved (compare Figs. 3 and 2), most probably due to cold electrons, trapped by the beam potential during the transient process when the self-potential decreases, as the energetic electrons leave the beam pulse to the walls. Experiments described in Ref. 30, where a filament was inserted into the beam path, reported the degree of neutralization to be about 90%. In the experimental studies in Ref. 29, the self-potential was measured for the case when a nearby

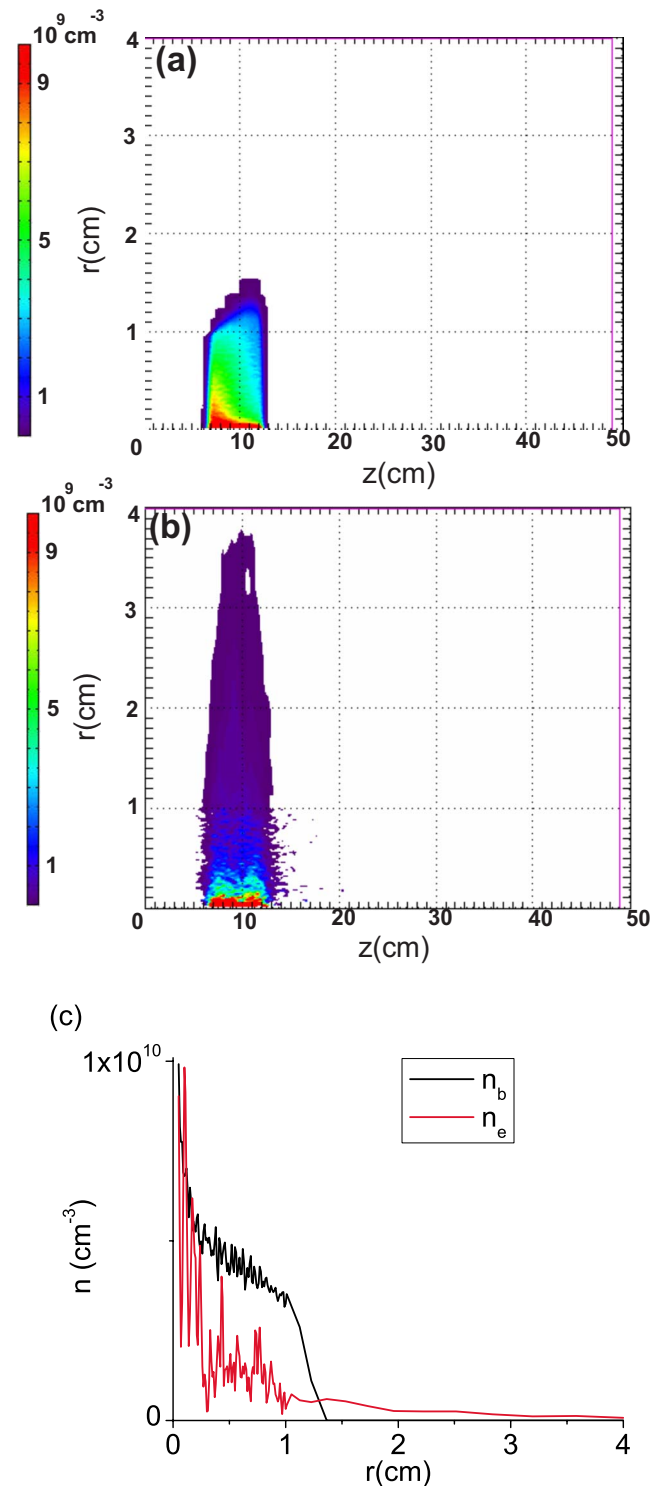


FIG. 2. (Color online) Color plots of (a) ion beam density, (b) electron density, and (c) one-dimensional slice plot along the radial direction ( $z=10$  cm) at 100 ns after beam propagation along the neutralizing chamber with emitting electrodes positioned at the sidewalls ( $r=4$  cm). Beam parameters are K<sup>+</sup> beam ions with energy 320 keV and beam pulse duration 44 ns (with 5 ns linear rise and decay times). The beam radial profile is taken to be Gaussian with  $n_{b0} \exp(-r^2/r_b^2)$  where  $r_b=1$  cm; and the maximum beam current density is  $0.19 \text{ A/cm}^2$ .

emitting wire (tantalum filament) was introduced into a long beam pulse at the edge of the beam. The measured potential drop from the center of the beam to the beam periphery was found to scale according to

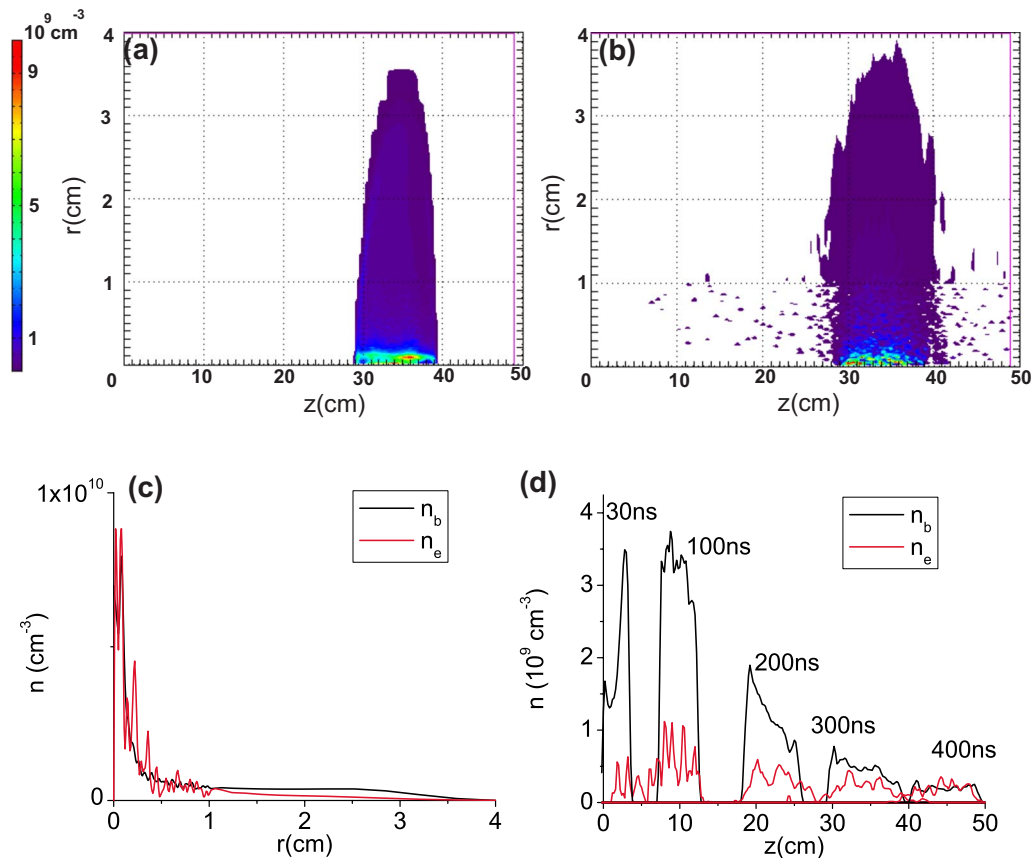


FIG. 3. (Color online) Color plots of (a) ion beam density, (b) electron density, and (c) one-dimensional slice plot along the radial direction ( $z=35$  cm) at 300 ns for the same conditions as in Fig. 2(d). One-dimensional plots of the ion beam density and electron density slice along the beam propagation direction at  $r=1$  cm for same conditions as in Fig. 2.

$$\Delta\phi = C\sqrt{\Delta\phi_0 T_e} e, \quad (6)$$

where  $\Delta\phi_0$  is the unneutralized beam potential,  $T_e$  is the emitter temperature, and  $C$  is a coefficient, whose value depends on the beam profile and location of the emitter. However, there has not been a sufficiently comprehensive theoretical and numerical studies performed to confirm the scaling given by Eq. (6).

In summary, neutralization by filament emission does not provide the necessary (close to the 99%) high degree of neutralization required by condition given in Eq. (4), and is not sufficient for space-charge neutralization of intense heavy ion beam pulses during drift compression.

## B. Neutralization by a grid immersed in the beam

If the emitting grid is immersed in the beam, the charge neutralization is greatly improved [compare Fig. 4(c) and Figs. 4(a) and 4(b)]. One way to accomplish this is to introduce a grid with high transmission ratio, e.g., a honeycomb grid structure in the path of the beam.<sup>34,35</sup> For the case of a high-energy beam, the emission may occur not only due to secondary electron emission, but also due to gas desorption and subsequent gas ionization by the beam without grid heating to achieve thermoemission. The results of numerical simulations for the emitting foil, transparent to the ion beam pulse, are shown in Figs. 4(c) and 5. In the simulations we have assumed intense emission from the emitting surfaces so

that the electron flux is limited by the Child–Langmuir law.<sup>33</sup>

In the experiments, some poor emitters may not provide a sufficient supply of electrons. As soon as the beam intersects the emitting foil, the beam space charge is well-neutralized, as shown in Fig. 5. However, recent experiments<sup>34</sup> with a honeycomb grid did not show significant neutralization when a honeycomb grid was introduced into the beam path in NDCX-I.<sup>36</sup> Neutralizing the beam space charge by means of biased grids or electrodes in the presence of a weak applied magnetic field ( $\sim 100$  G) allows the establishment of a focusing radial electric field in the transport section,<sup>37</sup> or serves as a high-current electrostatic plasma lens.<sup>38</sup> Emission from the grid inserted into the beam pulse may provide the necessary high degree of beam space-charge neutralization. However, there has not been a sufficiently comprehensive experimental study performed to confirm the high degree of neutralization.

## C. Neutralization by a plasma plug

Other options for neutralization include passing the beam pulse through a background plasma, either a finite size layer of plasma or a volumetric plasma produced everywhere along the beam path (see Fig. 1). Previous studies have explored the option of ion beam pulse neutralization by passing the beam pulse through a finite layer of plasma or a plasma plug.<sup>39</sup> The ion beam pulse extracts electrons from the

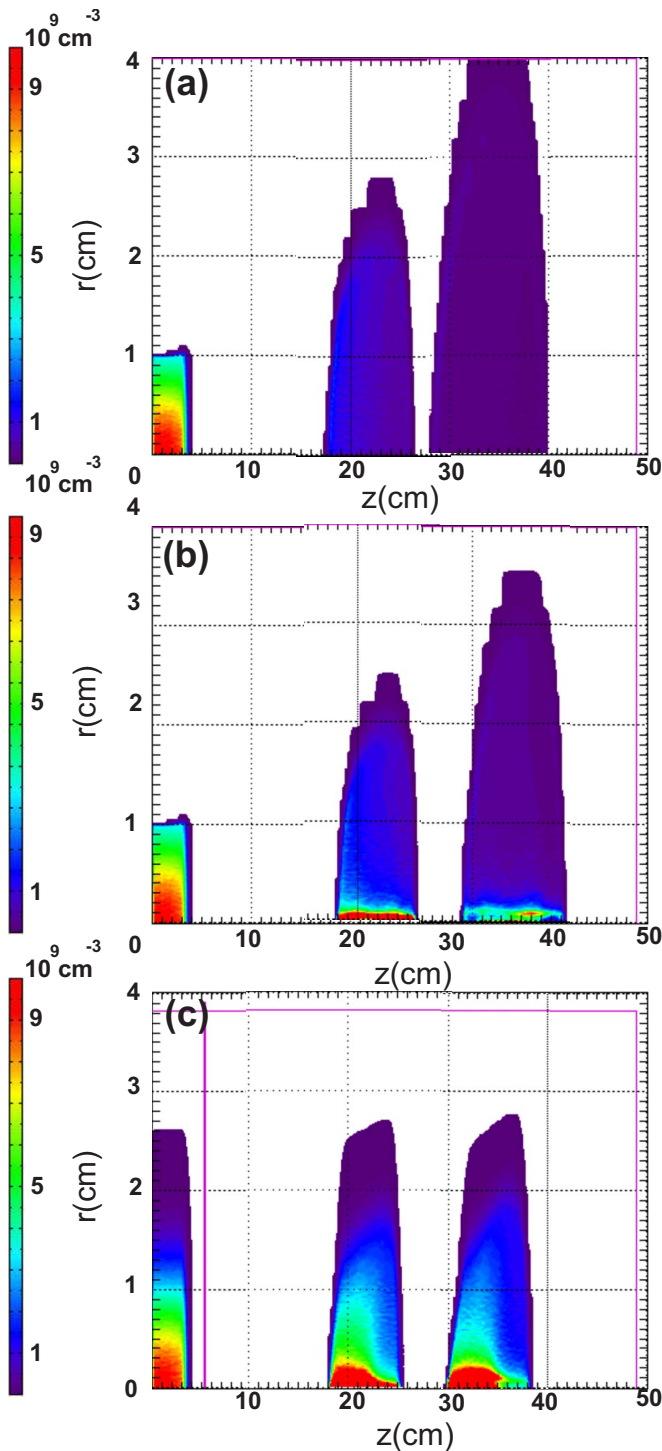


FIG. 4. (Color online) Color plots of ion beam density at three instants of time after beam propagation along the neutralizing chamber at 30, 200, and 300 ns. Comparison of the three cases: (a) unneutralized, (b) neutralized with emission from the sidewalls, and (c) neutralized with emission from a grid introduced into the beam path at  $z=5.1$  cm. Emission is assumed to be space-charge limited according to the Child–Langmuir law.

plasma plug and drags electrons along during its motion outside the plasma plug region. There are several limitations of this scheme. When the intense ion beam pulse enters the plasma, the electrons stream into the beam pulse in the strong self-electric and self-magnetic fields, attempting to drastically reduce the ion beam space charge from an unneu-

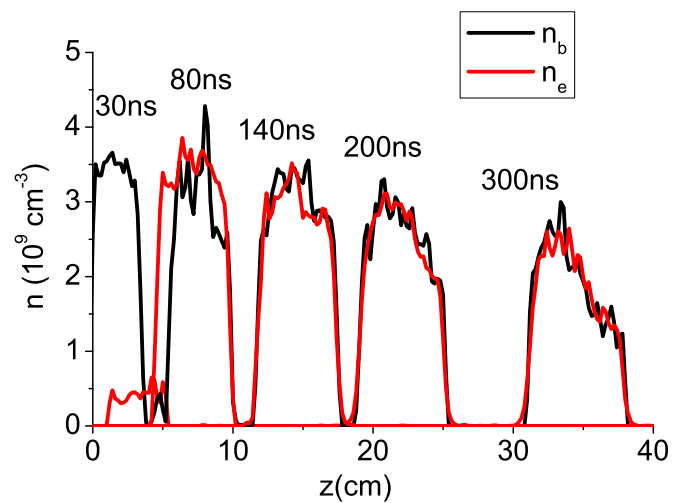


FIG. 5. (Color online) One-dimensional plots of the ion beam density and electron density slice along the beam propagation direction at  $r=1$  cm for the same conditions as in Fig. 4(c). Beam is very well space-charge neutralized after the beam passes through an emitting grid positioned at  $z=5.1$  cm.

tralized state to a completely neutralized state. After the ion beam pulse exits the plasma, the beam carries along the electrons, with average electron density and velocity equal to the ion beam's average density and velocity.<sup>40,41</sup> However, large-amplitude plasma waves are excited in a nonstationary periodic pattern resembling butterfly-wing motion.<sup>42</sup> Due to these transient effects, the beam may undergo transverse emittance growth, which would increase the size of the focal spot.<sup>21</sup> Smoother edges of the plasma plug density profile lead to a more gradual neutralization process and, in turn, results in a smaller emittance growth.<sup>21,22</sup> There are other limitations of this scheme in addition to a deterioration due to transient effects during the beam entry into and exit from the plasma plug. For typical plasma sources parameters with the electron temperature about 3–8 eV and density of order  $10^8$ – $10^{11}$   $\text{cm}^{-3}$ , the electron Debye length is small compared with the beam radius, providing a high degree of neutralization. After the ion beam exits the plasma plug it is focused by a magnetic lens. An accompanying electron beam extracted from the plasma plug follows the ion beam and is also transversely focused. Due to the radial compression of the electron beam, the transverse electron temperature increases inversely proportional to the beam radius-squared ( $T_e \sim 1/r^2$ ), and can reach very high values, in the keV range if the beam radius decreases by a factor of 10 during the radial compression.<sup>22</sup> Hot electrons cannot neutralize effectively the beam pulse at the focal spot because the electron Debye length becomes comparable with the beam radius. This may result in poor beam focusing. Including gas ionization by the beam ions improves the neutralization, but not to the level of 99% required for reliable ballistic drift compression, mainly because the electrons, which are produced by ionization, are concentrated in the beam path, whereas for best neutralization of the ion beam pulse, the supply of electrons should be from outside the beam<sup>21,22</sup> (see Sec. VI for details on the effects of gas ionization on the degree of beam current and charge neutralization). In view of these facts a

large volume background plasma is necessary everywhere along the beam path in order to provide the required high degree of the beam space-charge neutralization.

#### D. Neutralization by a volumetric plasma

Neutralized ballistic focusing typically requires the presence of a background plasma in and around the beam pulse path for very good charge neutralization [the degree of neutralization is very close to unity,  $(1-f) \ll 1$ ]. Reference 22 showed that hot electrons cannot neutralize the beam well enough. Therefore, any electron heating due to beam-plasma interactions has to be minimized. The presence of cold, “fresh” plasma in the beam path provides the minimum space-charge potential and the best option for neutralized ballistic focusing. Experimental studies of ballistic transverse focusing have confirmed that the best neutralization results are achieved when volumetric plasma is used everywhere along the beam path to assure robust charge neutralization.<sup>43,16</sup> Hence, in the following we only study the case when a large amount of cold background plasma is available everywhere along the beam path.

### III. CRITICAL PLASMA PARAMETERS FOR EFFECTIVE CHARGE AND CURRENT NEUTRALIZATION

If the beam pulse propagates through a cold unmagnetized plasma, and the background plasma density is large compared with the beam density, the self-electric and self-magnetic fields of the beam pulse can be obtained by the use of linear perturbation theory.<sup>44</sup> The transport of relativistic electron beams through the background plasma has been studied in detail in various contexts.<sup>45,46</sup> Interaction of a stripped, pinched ion beam pulse with the plasma has also been discussed in Ref. 28, where the assumption of current neutrality was made in order to obtain self-consistent solutions for the self-electric and self-magnetic fields of the beam pulse. In previous studies,<sup>28</sup> we focused on the nonlinear case, where the plasma density,  $n_p$ , is comparable with or smaller than the beam density,  $n_b$ , and the degree of current neutralization is arbitrary. The results of the theory agree well with particle-in-cell simulations and thus confirm the analytical formulas for the general nonlinear case,  $n_p \sim n_b$ .<sup>47</sup> This section briefly reviews the major conclusions of that study and serves as basis for discussions of the additional effects of gas ionization, and solenoidal and dipole magnetic fields in subsequent sections.

In most applications, the background plasma electrons are cold—the electron thermal velocity is small compared with the direct beam velocity [Eq. (5)]. We also consider intense particle beams with beam radius large compared to the Debye length. If the electron temperature is about 3 eV and density of order  $10^{11} \text{ cm}^{-3}$ , typical for most plasma sources, the electron Debye length is very small compared with the beam radius and is irrelevant for considered effects here associated with electron flows in the return current. Therefore, due to the fast motion of the beam pulse through the plasma, a flow in the return current is generated in the plasma with the flow velocity comparable to the beam pulse velocity. The plasma flow in the return current is faster than

the electron thermal velocity and is responsible for the self-electric and self-magnetic fields inside the beam pulse, whereas the electron pressure term can be neglected, in contrast to the case of slow beam pulses. Particle-in-cell simulations show that in most cases the electron flow is laminar and does not become multistreaming. Thus, the cold electron fluid equations can be used for the electron description, and thermal effects are neglected in the present study. The electron fluid equations together with Maxwell’s equations comprise a complete system of equations describing the electron response to a propagating ion beam pulse. The electron cold-fluid equations consist of the continuity equation,

$$\frac{\partial n_e}{\partial t} + \nabla \cdot (n_e \mathbf{V}_e) = 0, \quad (7)$$

and the force balance equation,

$$\frac{\partial \mathbf{p}_e}{\partial t} + (\mathbf{V}_e \cdot \nabla) \mathbf{p}_e = -e \left( \mathbf{E} + \frac{1}{c} \mathbf{V}_e \times \mathbf{B} \right), \quad (8)$$

where  $-e$  is the electron charge,  $\mathbf{V}_e$  is the electron flow velocity,  $\mathbf{p}_e = \gamma_e m \mathbf{V}_e$  is the average electron momentum,  $m$  is the electron rest mass, and  $\gamma_e$  is the relativistic mass factor. Maxwell’s equations for the self-generated electric and magnetic fields,  $\mathbf{E}$  and  $\mathbf{B}$ , are given by

$$\nabla \times \mathbf{B} = \frac{4\pi e}{c} (Z_b n_b \mathbf{V}_b - n_e \mathbf{V}_e) + \frac{1}{c} \frac{\partial \mathbf{E}}{\partial t}, \quad (9)$$

$$\nabla \times \mathbf{E} = -\frac{1}{c} \frac{\partial \mathbf{B}}{\partial t}, \quad (10)$$

where  $\mathbf{V}_b$  is the ion beam flow velocity,  $n_e$  and  $n_b$  are the number densities of the plasma electrons and beam ions, respectively (far away from the beam  $n_e \rightarrow n_p$ ), and  $Z_b$  is the ion beam charge state. The plasma ions are assumed to remain stationary with  $\mathbf{V}_i = 0$ . The assumption of immobile plasma ions is valid for sufficiently short ion pulses with  $2l_b < r_b \sqrt{M/m}$ .<sup>24,25</sup> Here,  $r_b$  and  $2l_b$  are the ion beam radius and length, respectively, and  $M$  is the plasma ion mass.

#### A. Criterion for charge neutralization

In Refs. 28, 48, 42, and 49 the steady-state propagation of an ion beam pulse propagating through a background plasma has been thoroughly explored. We have developed reduced *nonlinear* models, which describe the stationary plasma disturbance (in the beam frame) excited by the intense ion beam pulse of the *final length*. The analytical results agree very well with the results of particle-in-cell simulations.<sup>47,24,25,48,42,49</sup> The model predicts very good charge neutralization (the degree of neutralization is very close to unity) during quasisteady-state propagation, provided the beam is nonrelativistic and the beam pulse duration  $\tau_b$  is much longer than the electron plasma period  $2\pi/\omega_{pe}$ , where  $\omega_{pe} = \sqrt{4\pi e^2 n_e/m}$ , i.e.,

$$\omega_{pe} \tau_b \gg 2\pi. \quad (11)$$

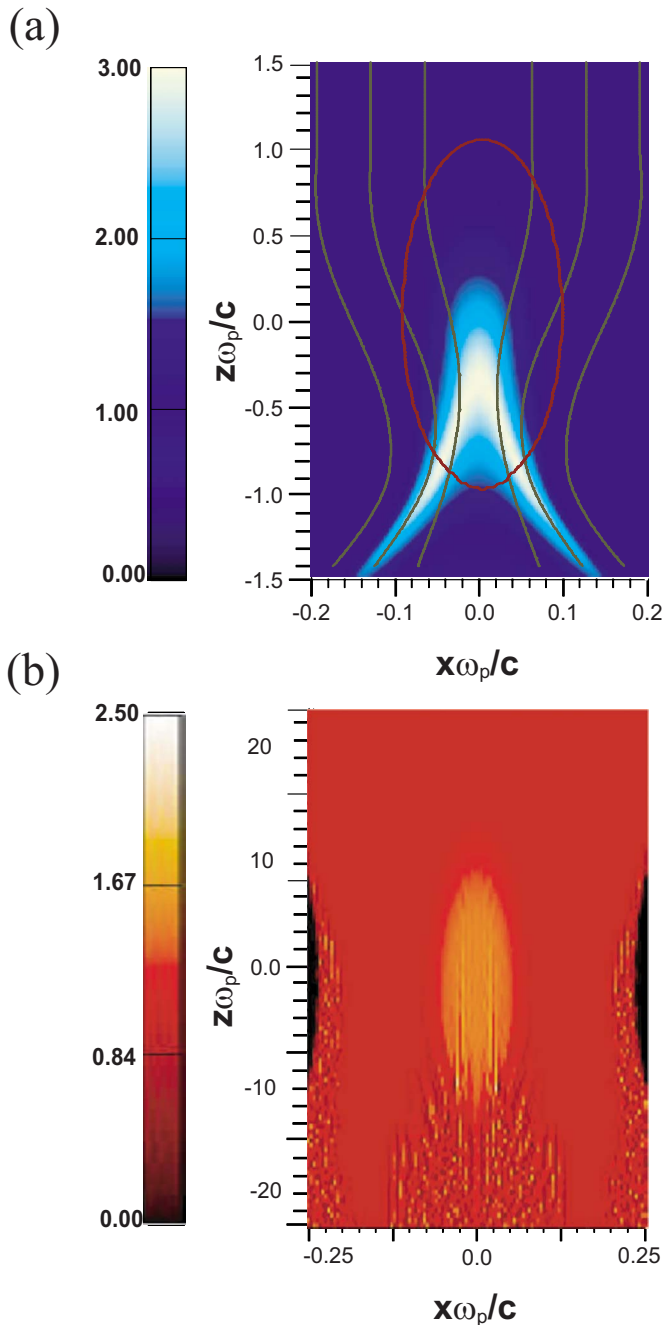


FIG. 6. (Color online) Color plots of the normalized electron density ( $n_e/n_p$ ); oval corresponds to the ion beam size; the grey lines corresponds to the electron trajectories in the beam frame for  $\beta_b=0.5$ ,  $l_b/r_b=10$ , and  $n_b/n_p=0.5$ , and (a)  $\omega_p\tau_b=4$  and (b)  $\omega_p\tau_b=60$ .

Thus, the degree of charge neutralization depends on the beam pulse duration and plasma density and is independent of the ion beam current (provided  $n_p > n_b$ ). Figure 6 shows the results of particle-in-cell simulations for electron density perturbations caused by propagation of a short ( $\omega_{pe}\tau_b=4$ ) and long ( $\omega_{pe}\tau_b=60$ ) ion beam pulses, and demonstrates that the charge neutralization is very good (the degree of neutralization is very close to unity) for long beam pulses. Quantitative formulas for the degree of neutralization are given in Sec. V.

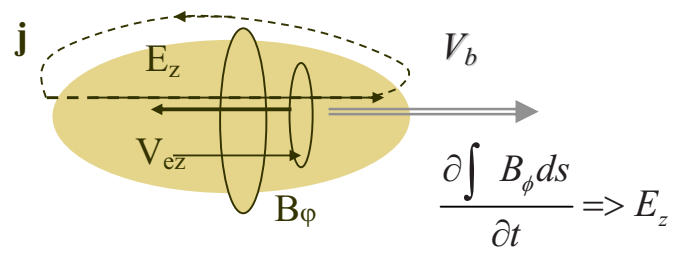


FIG. 7. (Color online) Schematic of return current generation by an alternating magnetic field in plasma.

## B. Criterion for current neutralization

The degree of ion beam current neutralization depends on both the background plasma density and the ion beam current. The ion beam current can be neutralized by the electron return current. The ion beam charge is neutralized primarily by the action of the electrostatic electric field. In contrast, the electron return current is driven by the inductive electric field generated by the inhomogeneous magnetic flux of the ion beam pulse in the reference frame of the background plasma<sup>28,49</sup> (see Fig. 7). The relationship between the electron flow velocity and the induced magnetic field can be obtained by applying the conservation of generalized vorticity,<sup>50</sup>

$$\mathbf{\Omega} \equiv \nabla \times \mathbf{p}_e - \frac{e}{c} \mathbf{B} = 0. \quad (12)$$

If  $\mathbf{\Omega}$  is initially equal to zero ahead of the beam, and all streamlines inside of the beam originate from the region ahead of the beam, then  $\mathbf{\Omega}$  remains equal to zero everywhere. Therefore, due to conservation of the generalized vorticity, it follows from Eq. (12) for long beam pulses with beam half length  $l_b \gg r_b$  that

$$B_\phi = -\frac{\partial A_z}{\partial r} \approx -\frac{c}{e} \frac{\partial p_{ez}}{\partial r}, \quad (13)$$

where  $B_\phi$  is the azimuthal component of self-magnetic field,  $A_z$  is the vector potential, and axisymmetry is assumed. Note that Eq. (13) also expresses the conservation of canonical momentum in the limit of long charge bunches,  $l_b \gg r_b$ , and

$$p_{ez} \approx \frac{e}{c} A_z, \quad (14)$$

if the plasma is unperturbed in front of the beam pulse, i.e.,  $\mathbf{V}_e=0$ ,  $\mathbf{A}=0$  ahead of the beam pulse. Equation (12) is valid even for short beam bunches, where the conservation of canonical momentum is not applicable.

The electron return current and self-magnetic field can be obtained from Ampere's law, provided the displacement current can be neglected. Substituting Eq. (14) into Ampere's law gives<sup>28,49,33</sup>

$$-\frac{1}{r} \frac{\partial}{\partial r} r \frac{\partial}{\partial r} A_z = \frac{4\pi}{c} Z_b e n_b V_{bz} - \frac{\omega_{pe}^2}{c^2} A_z. \quad (15)$$

Equation (15) describes the degree of current neutralization of the beam. Analyzing Eq. (15), one can see that the self-magnetic field of the beam pulse penetrates into the plasma

over distances of order the skin depth  $c/\omega_{pe}$ . If the beam radius  $r_b$  is small compared with the skin depth,  $r_b < c/\omega_{pe}$ , then the electron return current is distributed over distances of order  $c/\omega_{pe}$ , which is much broader than the ion beam current profile. The magnetic field far away from the beam should decrease to zero. Therefore, from Eq. (15) it follows that the total current integrated along the beam cross section over radial distances much larger than skin depth is equal to zero. From Ampere's law, it follows that the electron return current is about  $\omega_{pe}r_b/c$  times smaller than the ion beam current. Consequently, the ion beam current is neutralized by the electron current, provided the beam radius is large compared with the electron skin depth  $c/\omega_{pe}$ , i.e., provided

$$r_b > c/\omega_{pe}, \quad (16)$$

and is not neutralized in the opposite limit. This condition can be expressed as<sup>48,33</sup>

$$I_b > \frac{1}{4\gamma_b} I_A (n_b/n_p) = 4.25(\beta_b n_b/n_p) kA, \quad (17)$$

where  $\beta_b c$  is the directed ion beam velocity,  $\gamma_b = \sqrt{1/(1-\beta_b^2)}$ , and the Alfvén current,  $I_A = mc^3 \beta_b \gamma_b / e = 17\beta_b \gamma_b kA$ . The condition in Eq. (17) can be recast in terms of the Budker parameter for the beam,  $\nu_b = e^2 2\pi \int_0^\infty n_b r dr / M_b c^2$  using the relationship  $I_b/I_A \approx \nu_b M_b / m \gamma_b$ .<sup>51,52</sup>

#### IV. SELF-ELECTRIC FIELD AND SELF-FOCUSING FORCE OF THE FAST ION BEAM PULSE PROPAGATING THROUGH A BACKGROUND PLASMA

The self-force  $F_r(r)$  acting on the beam ions is often represented by introducing the degree of charge neutralization,  $f$ , and current neutralization,  $f_M$ ,<sup>12,23,48,51</sup> i.e.,

$$F_r(r) = \frac{4\pi e^2 Z_b^2}{r} \left[ (1-f) \int_0^r n_b r dr - (1-f_M) \beta_b^2 \int_0^r n_b r dr \right]. \quad (18)$$

However, for the case of ion beam propagation through a dense background plasma, the degree of charge neutralization is very close to unity, and the use of Eq. (18) is inconvenient. The electrons neutralize the ion beam pulse to such a high degree that the remaining self-electric field is small and is associated with the electron inertia terms caused by the electron flow in the return current,  $V_e \sim V_b n_b / n_p$ . Notwithstanding the fact that the electron inertia terms are small, the electron inertia terms are large compared with electron pressure effects for the case of fast beams, provided that the criterion in Eq. (5) is satisfied. For heavy ion fusion applications, we are primarily interested in *nonlinear* models, where the beam density is comparable with the plasma density and describe the plasma disturbance excited by an intense (finite length) ion beam pulse. For this case, the simplest way to analyze the self-electric field and self-focusing force of the ion beam pulse propagating in a background plasma is to perform the calculations in the beam frame. For analyzing the electron response to the beam pulse, the beam propagation through background plasma can be considered as a

steady-state phenomena because in most applications ion beam dynamics is slow compared with the electron response time. Therefore, the magnetostatic and electrostatic approximations

$$\mathbf{E}^b = -\nabla\phi^b, \quad (19)$$

are adequate.<sup>53</sup> Here, superscript  $b$  denotes the beam frame, as apposed to the laboratory frame. No subscripts or superscripts are used to denote values in the laboratory frame. From Eq. (3), the self-electric field can be obtained from the electron flow velocity in the electron return current, which gives

$$eE_z^b = m(V_b - V_{ez}) \frac{\partial V_{ez}}{\partial z}. \quad (20)$$

Here, we have neglected small radial terms in the limit of long beam pulses,  $l_b \gg r_b$  and  $V_{ez}$  is given by Eqs. (14) and (15).<sup>28</sup> From Eq. (20) it follows that the electrostatic potential is

$$e\phi_z^b = -m(V_b V_{ez} - V_{ez}^2/2), \quad (21)$$

and the radial self-electric field is given by

$$eE_r^b = m(V_b - V_{ez}) \frac{\partial V_{ez}}{\partial r}. \quad (22)$$

In the beam frame, the magnetic force acting on beam ions vanishes, and the total radial force is<sup>28</sup>

$$F_r = Z_b e E_r^b = m Z_b (V_b - V_{ez}) \frac{\partial V_{ez}}{\partial r}. \quad (23)$$

Equation (23) together with Eqs. (14) and (15) for the electron flow velocity in the electron return current, and the quasineutrality condition  $n_e = n_p + Z_b n_b$ , determine the self-focusing force. Note that this model is valid in the general nonlinear case where the background plasma density is comparable with the beam density,  $n_p \sim Z_b n_b$ , or even in the limit of tenuous plasma,  $n_p < Z_b n_b$ .<sup>28</sup> The self-focusing force is strongly affected by electron inertia effects. However, this force can also be important for fast, narrow ion beam pulses.

In the case of complete current neutralization,  $Z_b n_b V_b = n_e V_e$  and  $n_p \gg Z_b n_b$ , Eq. (23) becomes

$$F_r = \frac{m V_b^2 Z_b^2}{n_p} \frac{\partial n_b}{\partial r}. \quad (24)$$

Increase in the plasma density results in a decrease in the self-focusing force. Therefore, the pinching effect can be mitigated by introducing more plasma into the beam transport region. Note again, for fast ion beams, that adding finite electron temperature effects yields a small correction due to the electron pressure, i.e.,

$$F_r = \frac{Z_b^2 (m V_b^2 - T_e)}{n_p} \frac{\partial n_b}{\partial r},$$

according to Eq. (5).

It is instructive to describe self-electric field in the laboratory frame because most simulations are performed in the laboratory frame, where physical boundaries are stationary. In the laboratory frame, the self-electric field is given by

$$\mathbf{E} = \mathbf{E}^b - \frac{\mathbf{V}_b \times \mathbf{B}}{c}. \quad (25)$$

Here, the  $z$ -component of the electric field is the same in both the laboratory and beam frames, but the radial component is different, i.e.,

$$E_r = E_r^b + \frac{1}{c} V_b B_\phi. \quad (26)$$

Substituting Eqs. (22) and (14) into Eq. (26), it follows that the terms  $E_r^b$  and  $(1/c)V_b B_\phi$  nearly cancel each other, and the remaining small nonlinear term (proportional to  $Z_b n_b/n_p$ ) gives the radial self-electric field

$$eE_r = -mV_{ez} \frac{\partial V_{ez}}{\partial r}. \quad (27)$$

Note that the radial self-electric field in the laboratory frame is positive (defocusing), whereas the electric field in the beam frame is negative [compare Eqs. (20) and (15)]. Moreover, the radial self-electric field vanishes completely in the linear approximation (in the limit  $l_b \gg r_b$ ).<sup>28</sup> The electric field in the laboratory frame can be represented as a sum of the inductive and electrostatic parts<sup>28</sup>

$$\mathbf{E} = -\frac{1}{c} \frac{\partial}{\partial t} \mathbf{A} - \nabla \varphi, \quad (28)$$

where both the vector potential and the electrostatic potential can be expressed as functions of the flow velocity in the return current,<sup>28</sup>  $\mathbf{A} = cmV_{ez} \mathbf{e}_z$  and  $\varphi = mV_{ez}^2/2$ . Correspondingly, the  $z$ -component of the electric field in the laboratory frame is dominated by *the inductive part*, whereas the radial component is given by *the electrostatic part* of the electric field. That is, an electromagnetic code is required to describe the self-focusing force in the laboratory frame; and an electrostatic code is not sufficient, even for the case of a nonrelativistic beam and a weak self-magnetic field.

The self-focusing force in the laboratory frame can be expressed as<sup>28</sup>

$$F_r = eZ_b \left( E_r - \frac{V_{bz} B_\phi}{c} \right), \quad (29)$$

and is dominated by the magnetic component of the force. In Eq. (29),  $E_r$  is given by Eq. (27), and  $V_{ez}$  and  $B_\phi$  are given by Eqs. (14) and (15).

## V. THE DEGREE OF CHARGE NEUTRALIZATION AND EFFECTIVE PERVEANCE OF THE NEUTRALIZED FAST ION BEAM PULSE PROPAGATING THROUGH BACKGROUND PLASMA

The degrees of charge and current neutralization can be calculated by making use of Eqs. (14), (15), (27), and (29) and depend on the radial profile of the beam density. Analytical formulas have been developed in Ref. 48. Here, we focus on nonrelativistic, space-charge-dominated beams, which have a flat-top radial density profile with a sharp boundary at the outer beam radius,  $r_b$ . It is convenient to introduce the average degree of charge neutralization  $\langle f \rangle$  over the beam cross section defined by

$$\langle f \rangle = 1 - \frac{2 \int_0^{r_b} (Z_b n_b + n_p - n_e) r dr}{Z_b n_b r_b^2}. \quad (30)$$

Making use of Poisson's equation, we obtain from Eq. (30)

$$\langle f \rangle = 1 - \frac{E_r(r_b)}{2\pi e Z_b n_b r_b}. \quad (31)$$

The general expression for  $\langle f \rangle$  for arbitrary ratios of  $n_b/n_p$  and  $r_b \omega_{pe}/c$  is given in Ref. 48. In the limits  $n_b/n_p \ll 1$  and  $r_b \omega_{pe}/c \gg 1$ , it reduces to

$$\langle f \rangle = 1 - \beta_b^2 \frac{Z_b n_b}{n_p} \frac{c}{r_b \omega_{pe}}. \quad (32)$$

It can be readily shown<sup>48</sup> that the maximum deviation from quasineutrality occurs when  $r_b \sim c/\omega_{pe}$ , and the degree of nonquasineutrality is bounded by  $(Z_b n_b + n_p - n_e)/(Z_b n_b) < 0.25\beta_b^2$ . Therefore, for nonrelativistic, long ion beam pulses, there is almost complete charge neutralization. For heavy ion fusion parameters,  $\beta_b < 0.2$  and degree of charge neutralization are more than 99%.

The effective electric self-field perveance in the presence of plasma scales as  $1 - \langle f \rangle$ , where  $\langle f \rangle$  is the average charge neutralization defined in Eq. (32). Moreover, the *total* effective perveance including both self-electric and self-magnetic effects scales as<sup>12</sup>

$$\frac{Q_{\text{eff}}}{Q_0} = \frac{1 - \langle f \rangle - \beta_b^2 [1 - f_m(r_b)]}{1 - \beta_b^2}, \quad (33)$$

where the magnetic neutralization  $f_m(r_b) = -I_e(r_b)/I_b(r_b)$  is calculated at the beam edge, and  $I_e(r)$  is the electron current,  $I_e(r) = -e \int_0^r n_e V_{ez} 2\pi r dr$ , and  $I_b(r)$  is the ion beam current,  $I_b(r) = Z_b e \int_0^r n_b V_{bz} 2\pi r dr$ , both within radius  $r$ . The general expression for  $Q_{\text{eff}}$  for arbitrary ratios of  $Z_b n_b/n_p$  and  $r_b \omega_{pe}/c$  is given in Ref. 48. In the limits,  $Z_b n_b/n_p \ll 1$  and  $r_b \omega_{pe}/c \gg 1$ , it reduces to

$$Q_{\text{eff}} = -\frac{m_e Z_b n_b r_b \omega_{pe}}{M n_p 2c}. \quad (34)$$

The effective perveance  $Q_{\text{eff}}$  in Eq. (34) has a different sign for the perveance than Olson's electrostatic result<sup>31</sup> for a plasma plug,  $Q_e = Z_b m_e/M$ . The effective perveance in Eq. (34) is greatly reduced for the case of beam propagation in dense plasma with  $n_p \gg Z_b n_b$ .

## VI. EFFECTS OF GAS IONIZATION ON THE DEGREE OF BEAM CURRENT AND CHARGE NEUTRALIZATION

Gas ionization can considerably affect the degree of beam current neutralization. In the case of a preformed background plasma, the electric field accelerates electrons in the head of the beam pulse to produce the return current, and then decelerates electrons in the tail of the beam pulse to remove the return current behind the beam pulse. The radial electric field pushes electrons toward the beam center, and is compensated by the magnetic part of the Lorentz force  $eV_{ez} B_\phi/c$  (see Fig. 8). If an electron is produced inside the beam pulse in the tail region, then the longitudinal electric

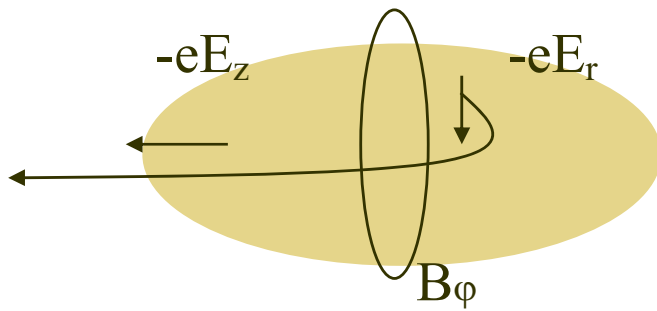


FIG. 8. (Color online) Schematic of the generation of a current wake behind an ion beam pulse due to gas ionization.

field accelerates such an electron in the opposite direction to the main flow of electrons comprising the background plasma. Moreover, the radial electric field pushes such electrons into the beam center because their force is not now compensated by the self-magnetic part of the Lorentz force  $eV_{ez}B_\phi/c$ . As a result, a wake in the electron flow velocity appears behind the ion beam pulse. Electrons flow in the direction opposite to the beam velocity in this wake region (see Fig. 9). In this case, the current associated with such electrons *enhances* the beam current rather than diminishes the beam current, as in the usual case for a self-generated return current. An analytical description of the return current when ionization effects need to be taken into account becomes complicated because the value of the return current is not only a function of the local plasma density and vector

potential, but is also determined by the entire preceding portion of the beam pulse.<sup>54</sup>

In summary, the effects of gas ionization can lead to considerable enhancement of the self-magnetic field in the tail of the beam pulse.

## VII. EFFECTS OF AN APPLIED SOLENOIDAL MAGNETIC FIELD ALONG THE BEAM PROPAGATION ON THE DEGREE OF CURRENT AND CHARGE NEUTRALIZATION

The application of a solenoidal magnetic field along the beam propagation allows additional control and focusing of the beam pulse.<sup>37</sup> Here, we consider the case when the ion beam pulse exits a diode located in vacuum, in a magnetic field free region, and enters a background plasma, separated from diode by an electrostatic field.<sup>9,10</sup> After propagating in a background plasma in the drift section for a few meters, the beam pulse is focused onto the target by a magnetic lens. A strong magnetic lens (final focusing magnet) with a magnetic field up to several Tesla can effectively focus an intense ion beam pulse in short distances of the order of a few tens of centimeters, as it is accomplished in the NDCX-I experiments.<sup>9,18</sup> However, due to the very strong magnetic field in the solenoid, the leaking of the magnetic field outside the solenoid can affect the degree of charge and current neutralization far away from the final focusing magnet. The plasma is produced by plasma sources inside the solenoidal magnetic field everywhere along the beam path in order to provide neutralization in the solenoid region. Even a small

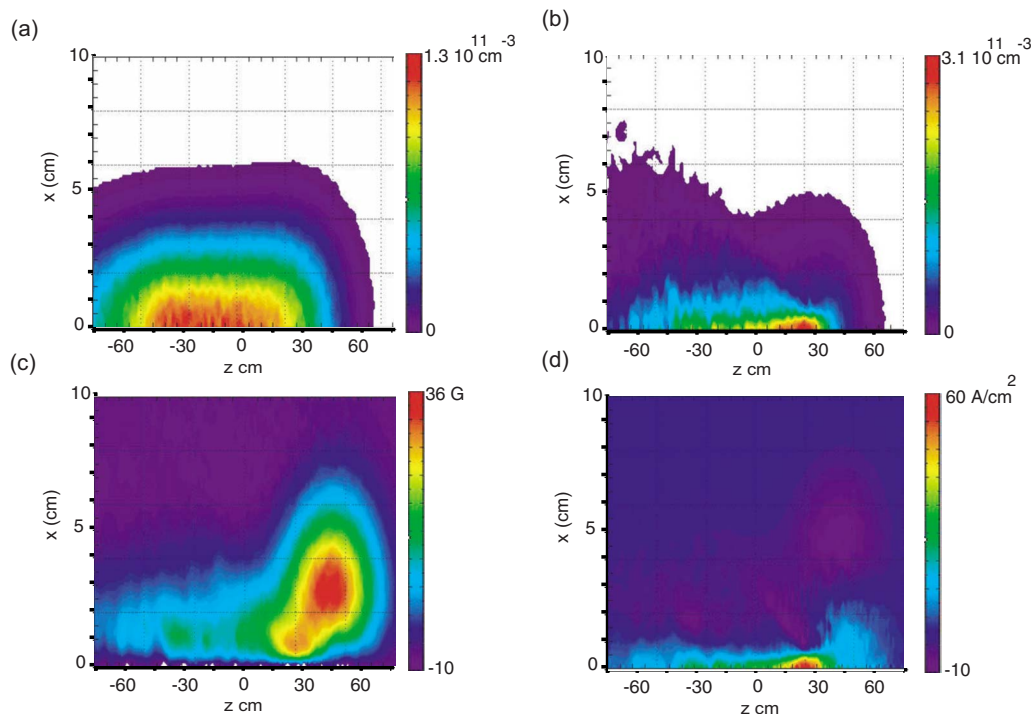


FIG. 9. (Color online) The electron density and ion density, magnetic field, and current density of the ion beam pulse are calculated in two-dimensional slab geometry using the LSP code (Ref. 22). The background plasma density is  $n_p=10^{11}$   $\text{cm}^{-3}$ . The beam velocity is  $V_b=0.2c$ ; the beam current is 1.2 kA ( $48.0$   $\text{A}/\text{cm}^2$ ), which corresponds to the ion beam density  $n_b=0.5n_p$ ; and the ion beam charge state is  $Z_b=1$ . The beam dimensions ( $r_b=2.85$  cm and  $\tau_b=1.9$  ns) correspond to a beam radius  $r_b=1.5c/\omega_{pe}$  and pulse duration  $\tau_b\omega_{pe}=75$ . Shown are color plots of (a) the ion density produced by beam ionization, (b) the electron density produced by beam ionization, (c) the magnetic field component  $B_y$  generated by the ion beam pulse, and (d) the current density.

solenoidal magnetic field, typically less than 100 G, strongly changes the self-magnetic and self-electric fields in the beam pulse propagating in a background plasma.<sup>27,63</sup> Such values of magnetic field can be present over distances of a few meters from the strong solenoid, and thereby affect the focusing of the beam pulse. Moreover, an additional small solenoidal magnetic field can be applied to optimize propagation of the beam pulse through a background plasma over long distances in the drift section.

Note that we are not relying on the collective lens effect proposed by S. Robertson,<sup>55</sup> where plasma or electron sources are absent inside the solenoidal magnetic field region, and neutralizing electrons are dragged by the ion beam pulse into the solenoid region, which is electron free in the absence of the beam pulse. For this case, the electrons cross the magnetic field lines, and thus a fast electron rotation with frequency  $\omega_{ce}/2$  is established inside the solenoidal magnetic field region. Here,  $\omega_{ce}=eB_z/mc$  is the electron cyclotron frequency. The magnetic force and centrifugal force yield a net focusing force acting on the electrons, i.e.,  $-e\omega_{ce}rB_z/2c+m\omega_{ce}^2r/4=-m\omega_{ce}^2r/4$ . The focusing force acting on the electrons is counterbalanced by the space-charge radial electric field  $eE_r=-m\omega_{ce}^2r/4$ , which in turn focuses the beam ions. For a collective lens to operate properly, no electrons should be present inside the solenoid.<sup>56</sup> Therefore, collective lens configurations have to be carefully designed to prevent electrons produced near the target from penetrating into the solenoid region.

Moreover, if an ion beam pulse propagates together with neutralizing, comoving electrons after exiting the plasma region, and encounters “fresh” new plasma, a very fast two-stream electron-electron instability is likely to develop; and the resulting electric field fluctuations will slow down the fast electrons comoving with the beam, and prevent them from following the beam pulse. If electrons comoving with the beam have a spread in velocity and are confined to the beam pulse by a positive potential,<sup>41,53</sup> as soon as the beam enters the background plasma, the self-potential is reduced and the fast electrons leave the beam pulse. Therefore, in the plasma region, electrons initially moving with the beam velocity cannot follow the beam pulse; and neutralization is provided by the “fresh” plasma electrons originating in front of the beam pulse. This phenomenon is observed in particle-in-cell simulations. Therefore, in the following we consider only the case where the beam propagates through fresh background plasma.

In Refs. 57 and 58, the response of a magnetized plasma to injection of an intense ion beam was studied while neglecting electron inertia effects, which corresponded to magnetic fields of a few Tesla in ion ring devices. In the present paper, we analyze the opposite limit, corresponding to small values of magnetic field. In the collisionless limit and without an applied solenoidal magnetic field, the return current is driven by an inductive electric field which is balanced by electron inertia effects. Taking electron inertia effects into account allows us to study the transition from the limit where the solenoidal magnetic field is small, i.e., where the presence of the applied solenoidal magnetic field begins to affect the return current in the plasma, and determines the range of

magnetic field values that strongly affect the self-electric and self-magnetic fields of a beam pulse propagating in a background plasma. This allows us to study the beam pulse evolution over a wide range of solenoidal magnetic field strengths, from approximately zero, to very large values, such as when the beam pulse encounters an applied solenoidal magnetic lens.

In Refs. 24 and 25 it was shown that application of a solenoidal magnetic field strongly affects the degree of current and charge neutralization when

$$\omega_{ce} > \omega_{pe}\beta_b, \quad (35)$$

or equivalently,

$$B > 320 \text{ G } \beta_b \sqrt{n_p/10^{10} \text{ cm}^{-3}}. \quad (36)$$

The threshold value of B given in Eq. (36) corresponds to relatively small values of the magnetic field for nonrelativistic beams. When the criterion in Eq. (36) is satisfied, application of the solenoidal magnetic field leads to three unexpected effects. The first effect is the dynamo effect, in which the electron rotation generates a self-magnetic field that is much larger than in the limit with no applied magnetic field. The second effect is the generation of a much larger self-electric field than in the limit with no applied field. The third unexpected effect is that the joint system consisting of the ion beam pulse and the background plasma acts as a paramagnetic medium if  $\omega_{ce} < 2\omega_{pe}\beta_b$ , i.e., the solenoidal magnetic field is enhanced inside of the ion beam pulse.

Application of the solenoidal magnetic field can be used for active control of beam transport through background plasma by enhancing or reducing the self-focusing force. Without the applied solenoidal magnetic field, the radial self-force is always focusing because the magnetic attraction of parallel currents in the beam always dominates the radial electric field, which is screened by the plasma better than the self-magnetic field. However, when a solenoidal magnetic field is applied, the radial electric force can become larger than the magnetic force, resulting in beam defocusing. For larger values of the solenoidal magnetic field, corresponding to

$$\omega_{ce} > 2\omega_{pe}\beta_b, \quad (37)$$

or equivalently,

$$B > 640 \text{ G } \beta_b \sqrt{n_p/10^{10} \text{ cm}^{-3}} \quad (38)$$

the beam generates whistler and lower hybrid waves.<sup>24,25,63</sup>

Note that here we are only interested in fast electron waves which modify the electron return current and not in slow waves and instabilities on the ion time scale. When whistler or lower hybrid waves are excited, the particle-in-cell simulations show that the structure of the self-electromagnetic field becomes rather complex, and the transport of very intense beam pulses can be strongly affected by the wave generation.<sup>20,59</sup> The intense whistler wave excitations can be used for diagnostic purposes.

In Ref. 63, it was also demonstrated, in the regime where  $\omega_{ce} \gg 2\beta_b\omega_{pe}$  and  $k_{qs}^{-1} \ll r_b \ll k_{em}^{-1}$ , where  $k_{em,qs}$  are given in Eq. (46), that the positive charge of the ion beam pulse becomes overcompensated by the plasma electrons, and the associated

strong transverse-focusing self-electric field has the dominant influence on the beam ions, compared with the self-magnetic field. It was also shown, for the case where the beam radius is small compared to the electron skin depth, that the self-focusing force is significantly enhanced compared to the self-focusing force acting on the beam particles in the absence of an applied magnetic field. In addition, the local diamagnetic plasma response is observed in the numerical simulations, and is also predicted analytically for  $\omega_{ce} \gg 2\beta_b \omega_{pe}$ . Note that these results differ significantly from the case  $\omega_{ce} < 2\beta_b \omega_{pe}$ , where the transverse electric field is defocusing, and the plasma response is paramagnetic. The qualitatively different local plasma responses are separated by the critical field case where  $\omega_{ce} = \omega_{ce}^{cr} = 2\beta_b \omega_{pe}$ , corresponding to the resonant excitation of large-amplitude wave-field perturbations. The threshold magnetic field in the inequality  $\omega_{ce} > 2\beta_b \omega_{pe}$  corresponds to a relatively weak magnetic field of the order of 10 G (for NDCX-I<sup>9,18</sup>) and 100 G (for NDCX-II<sup>19</sup>). Therefore, the magnetic fringe fields of the final-focus solenoid above this value can penetrate deep into the drift section. In particular, these fringe fields provide conditions for enhanced beam self-focusing, which can have a significant influence on the transverse beam dynamics for the parameters characteristic of NDCX-II.<sup>63</sup>

In the presence of an applied solenoidal magnetic field, the system of equations describing the self-electric and self-magnetic fields becomes much more complicated. A strong solenoidal magnetic field inhibits radial electron transport, and the electrons move primarily along the magnetic field lines. For high-intensity beam pulses propagating through a background plasma with pulse duration much longer than the electron plasma period, one is tempted to assume validity of the quasineutrality condition,  $n_e = n_p + Z_b n_b$ . In the limit of a strong applied solenoidal magnetic field, the plasma electrons are attached to the magnetic field lines, and their motion is primarily along the magnetic field lines. For one-dimensional electron motion, the charge density continuity equation,  $\partial \rho / \partial t + \nabla \cdot \mathbf{J} = 0$ , combined with the quasineutrality condition [ $\rho = n_p + Z_b n_b - n_e \approx 0$ ], yields zero net current,  $\mathbf{J} = 0$ . Therefore, in the limit of a strong solenoidal magnetic field, the beam current can be expected to be completely neutralized.

However, the preceding description fails to account for the electron rotation that develops in the presence of a solenoidal magnetic field. Due to the small inward radial electron motion, the electrons can enter into the region of smaller solenoidal magnetic flux. Due to the conservation of canonical angular momentum, the electrons start rotating with a very high azimuthal velocity (see Fig. 10). This electron rotation produces many unexpected effects.

#### A. Dynamo effect—enhancement of the self-magnetic and self-electric fields of the ion beam pulse due to application of weak solenoidal magnetic field

The first effect is the dynamo effect.<sup>60</sup> Under the conditions where electron magnetohydrodynamic equations can be used neglecting electron inertia terms, the magnetic field is attached to the electron flow.<sup>24,25,61</sup> Then, the electron rota-

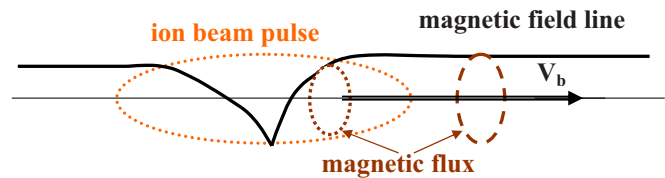


FIG. 10. (Color online) Schematic of perturbations of magnetic field lines in response to the propagating ion beam pulse. A small radial electron displacement generates a fast poloidal rotation. The poloidal rotation then twists the magnetic field and generates the poloidal magnetic field and large radial electric field.

tion bends the solenoidal magnetic field lines and generates an azimuthal self-magnetic field in the beam pulse. The dynamo effect remains if electron inertia effects are taken into account as well.<sup>24,25</sup> Moreover, the electron rotation can generate a self-magnetic field that is much larger than in the limit with no applied field. The second effect is the generation of a large radial electric field. Because the  $eV_{e\phi}B_z/c$  force should be balanced by a radial electric field, the electron rotation results in a plasma polarization, and produces a much larger self-electric field than in the limit with no applied solenoidal magnetic field. The total force acting on the beam particles now can change from always focusing in the limit with no applied solenoidal magnetic field, to defocusing at higher values of the solenoidal magnetic field. In particular, an optimum value of magnetic field for long-distance transport of an ion beam pulse, needed, for example, in inertial confinement fusion applications,<sup>62</sup> can be chosen where the forces nearly cancel. The third unexpected effect is that the joint system consisting of the ion beam pulse and the background plasma acts as a paramagnetic medium, i.e., the solenoidal magnetic field is enhanced inside of the ion beam pulse.

In order to quantify the above-mentioned effects, the system of Maxwell equations, Eqs. (9) and (10) and the electron fluid equations, Eqs. (7) and (8) have to be solved taking into account electron rotation and corresponding perturbation of the applied solenoidal magnetic field  $\delta B_z = \partial(rA_\phi)/r\partial r$ . The displacement current is small compared to the electron current, and Ampere's equations take the form

$$-\frac{1}{r}\frac{\partial}{\partial r}\left(r\frac{\partial A_z}{\partial r}\right) = \frac{4\pi e}{c}(Z_b n_b V_b - n_e V_{ez}), \quad (39)$$

$$\frac{\partial}{\partial r}\left(\frac{1}{r}\frac{\partial(rA_\phi)}{\partial r}\right) = \frac{4\pi e}{c}n_e V_{e\phi}, \quad (40)$$

where  $V_{e\phi}$  is the azimuthal component of the electron velocity. The electron flow velocity can be found using the conservation of the generalized vorticity,

$$\left(\frac{\partial}{\partial t} + \mathbf{V}_e \cdot \nabla\right)\left(\frac{\mathbf{\Omega}}{n_e}\right) = \left(\frac{\mathbf{\Omega}}{n_e} \cdot \nabla\right)\mathbf{V}_e, \quad (41)$$

where the generalized vorticity is defined by  $\mathbf{\Omega} = \nabla \times (m\mathbf{V}_e - e\mathbf{A}/c)$ . Projecting Eq. (41) along the longitudinal and azimuthal axes, we readily obtain<sup>24,25</sup>

$$V_{ez} = \frac{e}{mc} A_z - \frac{B_0}{4\pi m V_b n_e} \frac{1}{r} \frac{\partial(rA_\phi)}{\partial r}, \quad (42)$$

$$V_{e\phi} \left( 1 + \frac{\omega_{ce}^2}{\omega_{pe}^2} \right) = \frac{e}{mc} A_\phi - \frac{B_0}{4\pi m V_b n_e} \frac{\partial A_z}{\partial r}. \quad (43)$$

In deriving Eqs. (42) and (43), it has been taken into account that in the linear approximation,  $n_b \ll n_e$ , the radial component of the equation for the electron momentum gives  $E_r = -V_{e\phi} B_0 / c$ . Furthermore use has been made of Poisson's equation.<sup>24,25</sup> The last term on the right-hand side of Eq. (42) describes the magnetic dynamo effect, i.e., the generation of a self-magnetic field due to rotation ( $B_\phi \sim B_z V_{e\phi} / V_{ez}$ ). The last term on the right-hand side of Eq. (43) describes the generation of electron rotation due to the radial displacement caused by a not fully compensated current and remnant self-magnetic field. The second term inside the parenthesis on the left-hand side of Eq. (43) describes the departure from quasineutrality condition.<sup>24,25</sup> Figure 11 shows very good agreement between analytical theory and the PIC simulation results. Enhancement in the self-magnetic field (factor of 3) and self-electric field (factor of 10) produced by the ion beam pulse due to the application of a weak solenoidal magnetic field is shown. The paramagnetic effect of the enhanced solenoidal magnetic field inside of the ion beam pulse is also evident. The maximum enhancement is observed when  $\omega_{ce} \rightarrow 2\omega_{pe}\beta_b$ . However, in this range of the applied solenoidal magnetic field, whistler waves are excited, and the structure of the self-magnetic field becomes more complicated. Moreover, the slice approximation for long thin beams used in Eqs. (42) and (43) is not valid when the waves are excited by the beam<sup>24,25</sup> in the regime

$$\omega_{ce} > 2\beta_b \omega_{pe}. \quad (44)$$

In this case, the slice approximation is not valid because the profiles for the self-electric and self-magnetic fields in the presence of a whistler wave excitation depend on the entire profile of the beam pulse and not only on the local cross section.<sup>63</sup>

### B. Whistler wave excitation and effects of self-focusing on ion beam propagation through a background plasma along a solenoidal magnetic field

If the condition in Eq. (44) is satisfied, whistler wave can be excited by the ion beam pulse. The whistler wave dispersion relation is<sup>63,64</sup>

$$\omega_{wh}^2 = \frac{k_x^2 k_z^2 \omega_{ce}^2}{[k_x^2 + \omega_{pe}^2/c^2][k_x^2(1 + \omega_{ce}^2/\omega_{pe}^2) + \omega_{pe}^2/c^2]}, \quad (45)$$

where the approximation of a long thin beam pulse has been assumed,  $k_x \gg k_z$ ,  $\omega \ll \omega_{ce}, \omega_{pe}$ , and the ion response is neglected. Whistler waves are in resonance with the ion beam pulse when their phase velocity coincides with the ion beam velocity,  $\omega_h(k_x, k_z) = k_z V_b$ . The necessary condition for resonance is given by Eq. (44) (see Fig. 12). The solution to Eq. (45) gives two values for the transverse wave number  $k_x$ , a small value  $k_{em}$  corresponds to long wavelength electro-

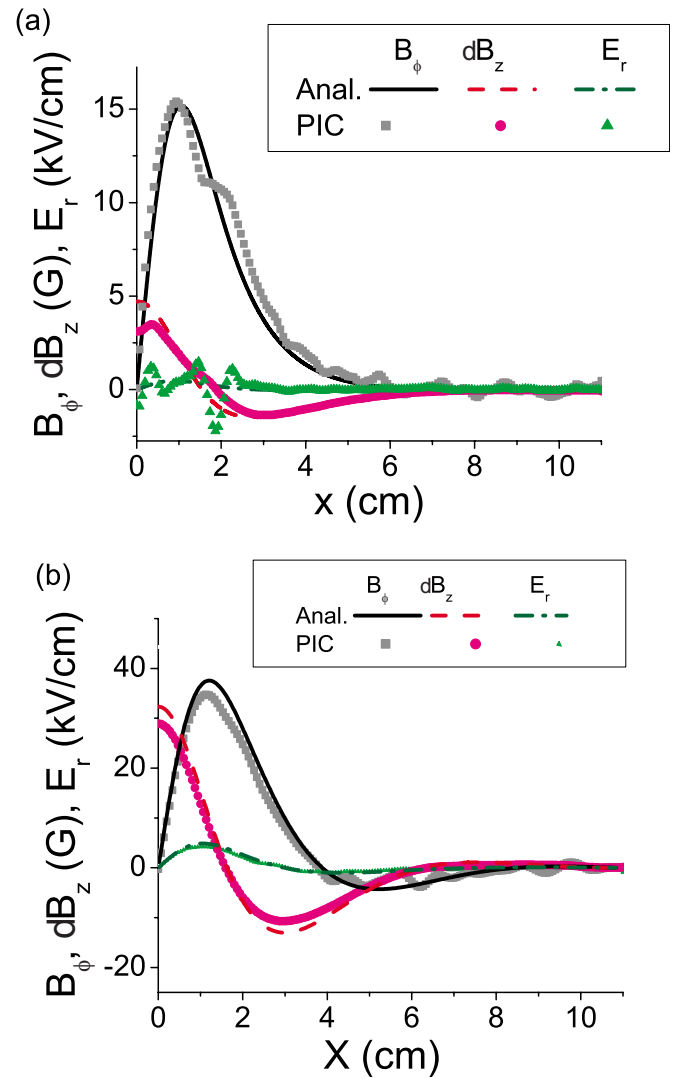


FIG. 11. (Color online) The azimuthal self-magnetic field, the self-magnetic field perturbation in the solenoidal magnetic field, and the radial electric field in a perpendicular slice of the beam pulse. The beam parameters are (a)  $n_{b0} = n_p/8 = 3 \times 10^{10} \text{ cm}^{-3}$ ,  $V_b = 0.33c$ , and the beam density profile is taken to be Gaussian with  $r_b = 1 \text{ cm}$ . The applied magnetic field is (a)  $B_{z0} = 300 \text{ G}$ ;  $c\omega_{ce}/V_b = 0.57$ , and (b)  $B_{z0} = 900 \text{ G}$ ;  $c\omega_{ce}/V_b = 1.7$ .

magnetic perturbations, and a high value  $k_{qs}$  corresponds to short wavelength electrostatic perturbations with

$$k_{em,qs}^2 = \frac{\omega_{pe}^2 \omega_{ce}^2 - 2\beta_b^2 \omega_{pe}^2 \mp \sqrt{\omega_{ce}^2 (\omega_{ce}^2 - 4\beta_b^2 \omega_{pe}^2)}}{2\beta_b^2 (\omega_{pe}^2 + \omega_{ce}^2)}. \quad (46)$$

As evident from Fig. 12, the group velocity,  $\partial\omega_{wh}/\partial k_z$  of the long wavelength electromagnetic perturbations is greater than the beam velocity, whereas the group velocity of the short wavelength electrostatic perturbations is smaller than the beam velocity. Therefore, long wavelength electromagnetic perturbations propagate ahead of the beam, whereas the short wavelength electrostatic perturbations lag behind the beam. Both waves have transverse group velocity  $\partial\omega_{wh}/\partial k_x$ . Hence, the waves also propagate sideways from the beam pulse. Typical results are shown in Fig. 13. Propagating in magnetized ionospheric or magnetospheric plasma, charged particle beams can excite whistler wave-field perturbations,

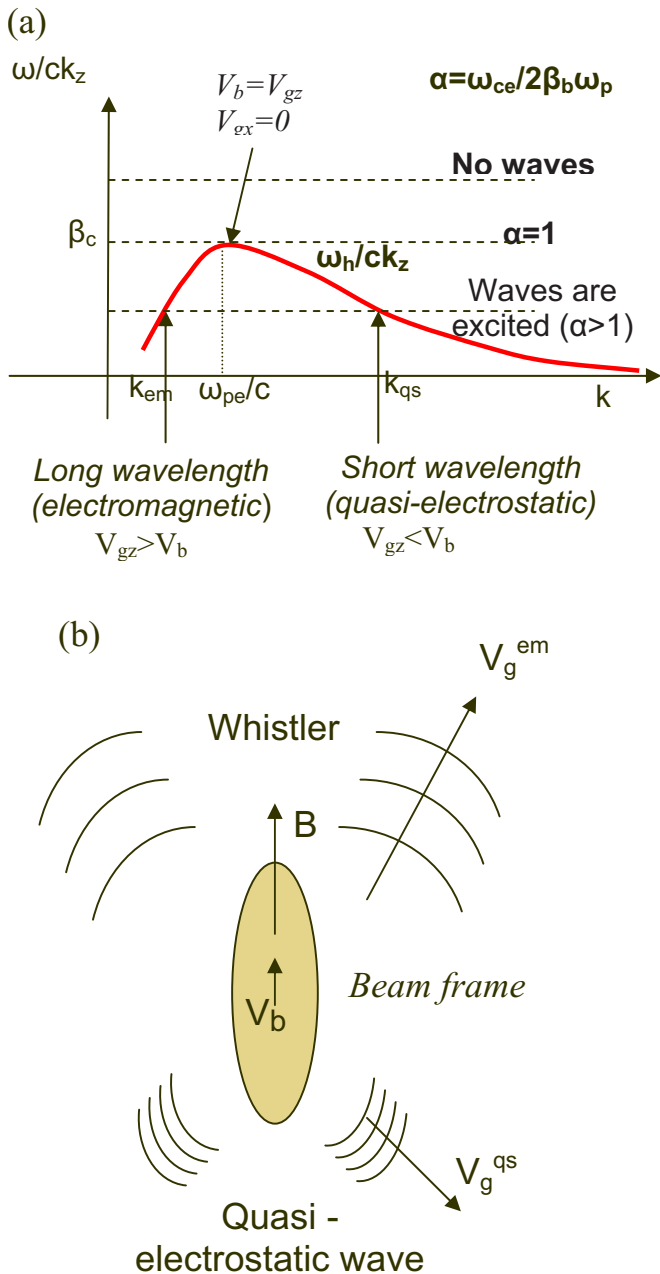


FIG. 12. (Color online) (a) The phase velocity of the whistler wave is plotted as a function of wave vector (solid curve) and is intersected by different values of the normalized beam velocity  $\beta_b$  (dashed lines). (b) Schematic illustration of the whistler waves excited by the ion beam pulse. In the beam frame of reference, the long-wavelength electromagnetic wave field propagates ahead of the beam pulse, and the short-wavelength electrostatic wave field lags behind the beam pulse.

and therefore can be used as compact on-board emitters in the very-low-frequency range, replacing large-apertures electromagnetic antennas.<sup>65,66</sup> Analytical and numerical studies of the whistler branch excitation by a density-modulated electron beam propagating through a background plasma along a uniform magnetic field, including linear and nonlinear effects, have been recently reported in Refs. 67–69 in the limit of a very thin ion beam,  $r_b \ll k_{qs}^{-1}$ . Reference 63 performed analytical calculations of whistler wave excitation in slab geometry. Analytical calculations have been verified by comparing with the results of particle-in-cell simulations,

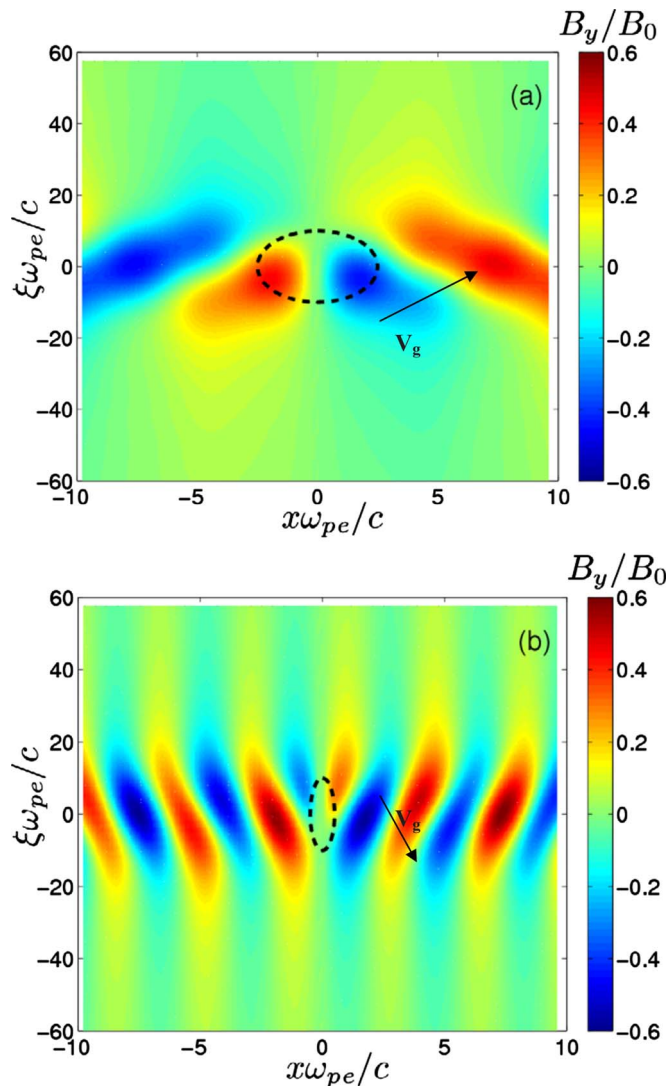


FIG. 13. (Color online) Plots of the steady-state amplitude of the transverse magnetic field perturbations  $B_y$ . The beam-plasma parameters correspond to  $Z_b=1$ ,  $l_b=10c/\omega_{pe}$ ,  $\beta_b=0.33$ , and  $n_p=2.4 \times 10^{11} \text{ cm}^{-3}$ . The applied magnetic field,  $B_z=1600 \text{ G}$ , corresponds to  $\omega_{ce}/(2\beta_b\omega_{pe})=1.54$ . The frames in the figure show (a) excitation of primarily long-wavelength electromagnetic waves by a wide-aperture ion beam with  $r_b=2.5c/\omega_{pe}$  and (b) excitation of primarily short-wavelength quasiolestatic waves by a thin beam with  $r_b=0.5c/\omega_{pe}$ . The normalization factor in (a) and (b) is given by  $B_0=4\pi n_{b0}Z_b e\beta_b r_b$ . The arrows schematically illustrate the direction of the wave packet group velocity. The dashed lines correspond to the contours of constant beam density corresponding to the effective beam radius  $r_b$ .

which showed very good agreement. Particle-in-cell simulations in cylindrical geometry were also carried out, and showed that the analytical formulas obtained for the self-focusing force can be applied in cylindrical geometry as well.

The analysis in Ref. 63 showed that wave excitation does not affect the self-focusing force in the limit of strong solenoidal magnetic field and not very thin beams, i.e.,

$$\omega_{ce} \gg 2\beta_b\omega_{pe} \quad \text{and} \quad r_b \gg k_{qs}^{-1} = (1 + \omega_{ce}^2/\omega_{pe}^2)^{1/2} \frac{\beta_b c}{\omega_{ce}}. \tag{47}$$

In this limit the degree of beam current neutralization is high. However, the self-magnetic field in the wave excitation can

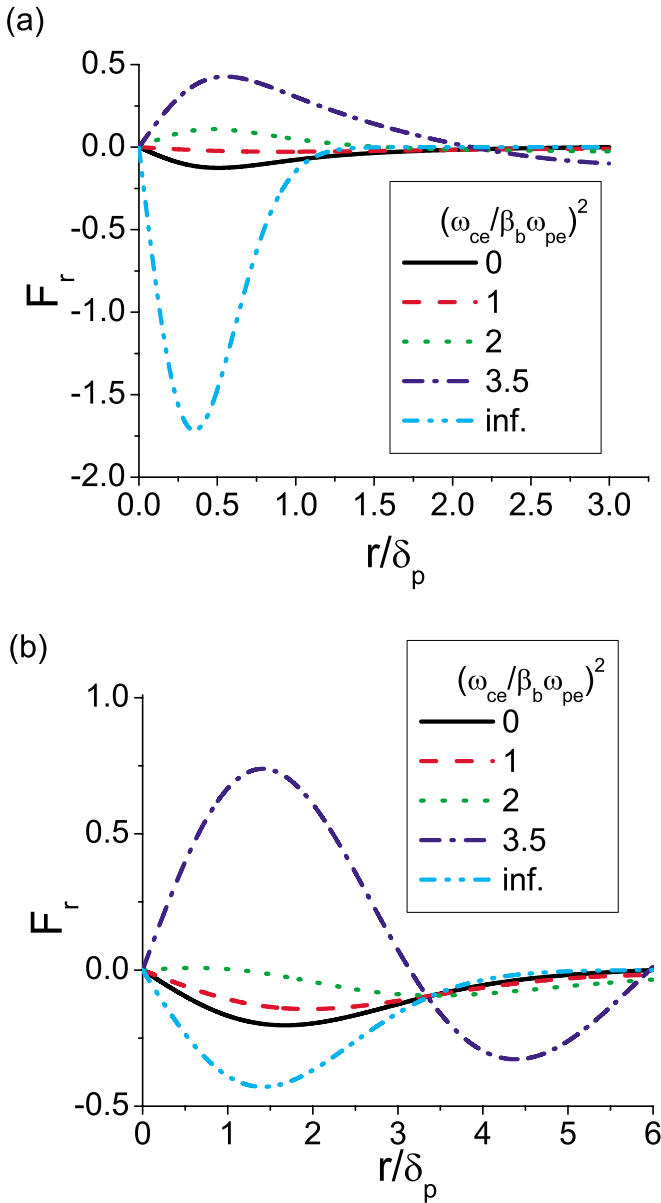


FIG. 14. (Color online) Plots of the normalized radial force acting on beam ions propagating through plasma for different values of  $(\omega_{ce}/\beta_b\omega_{pe})^2$  calculated from Eqs. (23)–(27) for  $(\omega_{ce}/\beta_b\omega_{pe})^2 < 4$  and Eq. (45) for  $(\omega_{ce}/\beta_b\omega_{pe})^2 \rightarrow \infty$ . The force is normalized to  $Z_b n_{b0} m V_b^2 \omega_{pe} / n_p c$  [see Eq. (36)]. The beam density profile is a Gaussian,  $n_{b0} \exp(-r^2/r_b^2)$  with (a)  $r_b = 0.5c/\omega_{pe}$  and (b)  $r_b = 2c/\omega_{pe}$ .

be comparable with the remaining self-magnetic field. Nevertheless, the total self-magnetic field is small, and does not influence the self-focusing force. Moreover, we can use Eq. (22) to determine the radial self-electric field in the beam frame. Because the self-magnetic field is well neutralized, the self-electric field in the laboratory frame,

$$E_r = E_r^b + \frac{1}{c} V_{bz} B_\phi \approx E_r^b, \quad (48)$$

is the same as in the beam frame and therefore is electrostatic. The self-focusing force acting on the beam ions is given by Eq. (24). Variation of the self-focusing force acting on beam ions as a function of applied magnetic is shown in Fig. 14.

### C. The degree of charge neutralization and effective perveance of the neutralized fast ion beam pulse propagating through background plasma along a solenoidal magnetic field

Substituting Eq. (22) for the radial self-electric field into Eq. (31) for the average degree of charge neutralization  $\langle f \rangle$  gives in the limit  $Z_b n_b / n_p \ll 1$ ,

$$\langle f \rangle \approx 1 + 2\beta_b^2 \frac{c^2}{r_b r_g \omega_{pe}^2}. \quad (49)$$

Here,  $r_g = n_b / |(\partial n_b / \partial r)|$  is the effective radial scale of the ion beam density profile at the beam edge. Note that the second term on the right-hand side of Eq. (49) is positive because in this regime electrons overcompensate positive ion charge and the radial electric field at the beam edge is negative. From Eq. (49), it is evident that the electric field increases and the degree of charge neutralization for the case  $r_b \ll c/\omega_{pe}$ .<sup>63</sup> Equation (49) can be used only for  $r_b, r_g \gg k_{qs}^{-1} = (1 + \omega_{ce}^2/\omega_{pe}^2)^{1/2} \beta_b c / \omega_{ce}$  and  $\omega_{ce} \gg 2\beta_b \omega_{pe}$ . The maximum deviation from quasineutrality occurs for the smallest possible beam radius and sharpest ion beam density gradients. As a function of the parameter  $\omega_{ce}/\omega_{pe}$ , the minimum value of  $k_{qs}^{-1} = \beta_b c / \omega_{pe}$  occurs when  $\omega_{ce} > \omega_{pe}$ . Substituting the values  $r_b \sim r_g \sim \beta_b c / \omega_{pe}$  into Eq. (49) one finds that  $\langle f \rangle \sim 2$ , and the beam can become non-neutralized, as observed in numerical simulations.<sup>24,25</sup> Therefore, even for nonrelativistic, long ion pulses, complete charge neutralization is not guaranteed in the presence of a solenoidal magnetic field, if  $r_b \approx r_g \sim \beta_b c / \omega_{pe}$ . However, for heavy ion fusion parameters,  $r_b \geq c/\omega_{pe}$  and  $\beta_b < 0.2$  and the degree of charge neutralization can exceed more than 99% by increasing the plasma density according to Eq. (49).

The effective self-electric perveance in the presence of plasma scales as  $1 - \langle f \rangle$ , where  $\langle f \rangle$  is the average charge neutralization defined in Eq. (32). Because the contribution to the self-focusing force by the self-magnetic field can be neglected in the limit  $\omega_{ce} \gg 2\beta_b \omega_{pe}$ , the total effective perveance including both self-electric and self-magnetic effects is given approximately by the self-electric perveance. Substituting Eq. (49) for  $\langle f \rangle$  into Eq. (33) gives for  $Q_{\text{eff}}$ ,

$$Q_{\text{eff}} \approx -\frac{m r_b Z_b^2 n_b}{M r_g n_p}. \quad (50)$$

The effective perveance in Eq. (50) can be greatly reduced for the case of beam propagation in dense plasma with  $r_b \gg c/\omega_{pe}$ .

### VIII. EFFECTS OF A DIPOLE MAGNETIC FIELD ACROSS THE BEAM PROPAGATION ON THE DEGREE OF CURRENT AND CHARGE NEUTRALIZATION

A dipole magnetic field can be used to deflect the beam. Due to the large ion beam space charge, it is necessary to fill the dipole region with a background plasma to neutralize the beam space charge. The question arises as to whether the plasma can still neutralize the ion beam space-charge density effectively. In this case, it is necessary to take into account the plasma flows in all directions simultaneously: along the dipole magnetic field, and across the magnetic field, in order

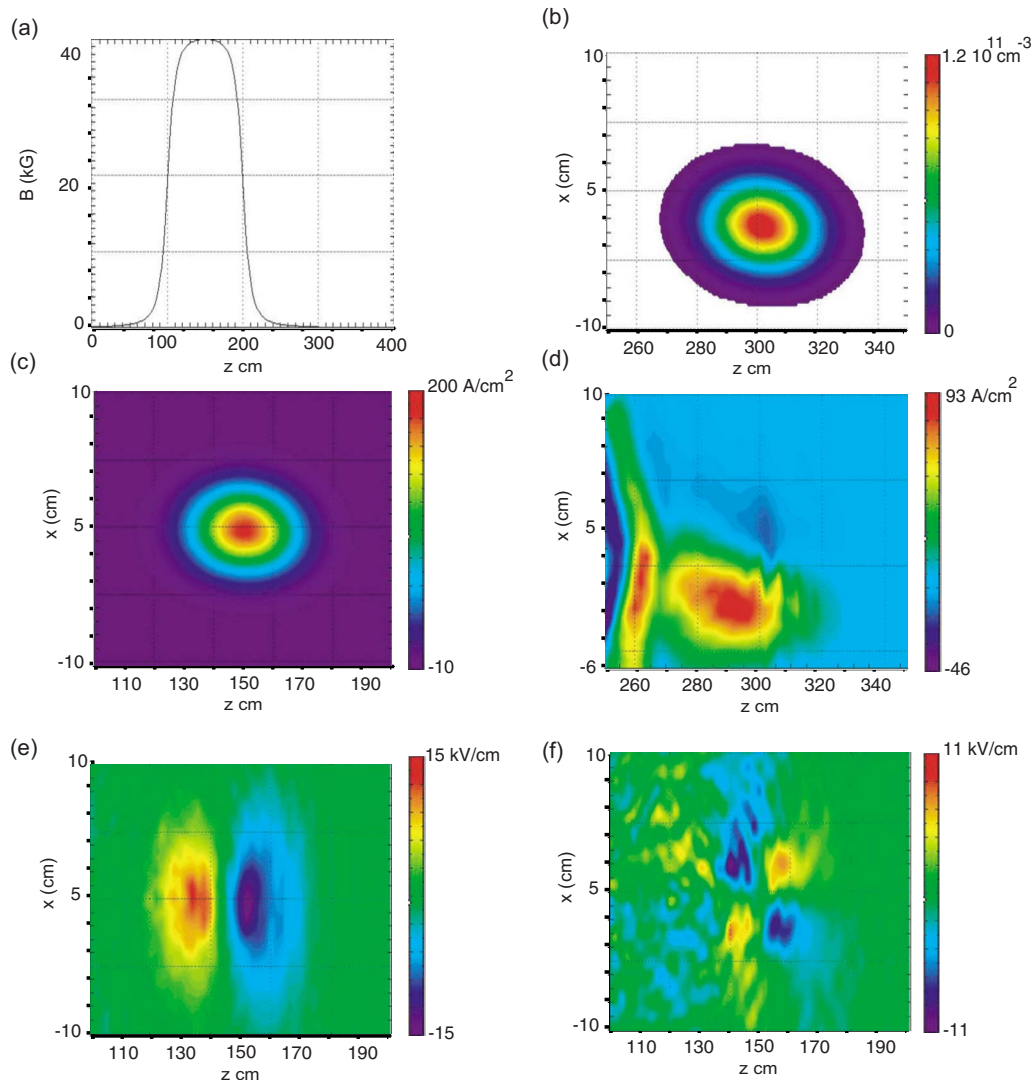


FIG. 15. (Color online) Beam propagation in a dipole magnetic field. Plots correspond to (a) the magnetic field  $B_y$  of the dipole, (b) the beam density in the dipole region, (c) the current density  $j_z$  in the dipole region, (d) the current density  $j_z$  outside the dipole region, (e) the longitudinal, inductive electric field  $E_z$ , and (f) the transverse electric field  $E_x$ . The background plasma density is  $n_p=10^{11} \text{ cm}^{-3}$ ; the beam velocity is  $V_b=0.2c$ ; the beam current is 1.2 kA (48.0  $\text{A/cm}^2$ ), which corresponds to the ion beam density  $n_b=0.5n_p$ ; and the ion beam charge state is  $Z_b=1$ . The beam dimensions ( $r_b=2.85 \text{ cm}$  and  $\tau_b=1.9 \text{ ns}$ ) correspond to a beam radius  $r_b=1.5c/\omega_{pe}$  and pulse duration  $\tau_b\omega_{pe}=75$ .

to properly take into account of all of the drifts and flows set up in a dipole magnetic field, when the beam pulse moves in background plasma. The neutralization of beams and propagating plasmoids across the magnetic field has been studied extensively both in simulations and experimentally, see e.g., Ref. 70 and references therein. Here, we discuss only the effects associated with the self-electric and self-magnetic fields of fast, intense ion beam pulses of finite length. Three-dimensional simulations show that the beam space-charge density is well-neutralized by the plasma flow along the dipole magnetic field (due to connection to the emitting sidewalls). However, because the electron motion across the magnetic field is greatly reduced by the dipole magnetic field, *the current is almost completely unneutralized*, as shown in Fig. 15. The unneutralized current generates a time-varying self-magnetic field in the laboratory frame, which in turn produces an inductive electric field  $E_z$ , as shown in Fig. 15(e). The longitudinal electric field  $E_z$  pro-

duces drifts in the  $x$ -direction and polarizes the plasma, as evident in Fig. 15(f). The transverse electric field in the  $x$ -direction has different signs for the beam head and the beam tail. After the beam exits the dipole region, the current becomes neutralized as shown in Fig. 15(d). However, some complex structures appear at the dipole boundary, as evident by comparing the color plots of the beam density in Fig. 15(b) and the current density in Fig. 15(d). Therefore, an intense ion beam can be effectively deflected by a dipole magnetic field directed perpendicular to the beam propagation direction. However, the self-magnetic field of the beam pulse is not neutralized by the plasma inside the dipole region, and a transverse electric field is generated due to the plasma polarization. This can result in a pinching effect and an unwanted emittance growth of the beam pulse. An additional comprehensive study needs to be performed in order to quantify these effects.

## IX. CONCLUSIONS

In this paper we have reviewed several neutralization schemes for intense ion beam pulses, including neutralization by emitting filaments positioned near the beam sides, neutralization by gas ionization, neutralization by a grid immersed in the beam, and neutralization by passing the beam pulse through a background plasma, either a finite size layer of plasma or a volumetric plasma produced everywhere along the beam path. All schemes except for neutralization by a volumetric plasma cannot provide the necessary very high degree of neutralization (>99%) required for ballistic drift compression of intense ion beam pulses. Therefore, neutralized ballistic focusing typically requires the presence of a background plasma in and around the beam pulse path for very good charge neutralization. Correspondingly, the main focus of this paper is on the neutralization of intense ion beam pulses by volumetric background plasma. In plasma sources, the electron temperature is about 3 eV, and the plasma density is of order  $10^{11} \text{ cm}^{-3}$ . For these plasma parameters, the electron Debye length is very small compared with the beam radius, and the electrons neutralize effectively the ion beam space charge. Due to the fast motion of the beam pulse through the background plasma, a return current is generated in the plasma, in which the electron flow velocity is comparable with the beam velocity. Thus the electron flow in the return current is faster than the thermal electron velocity, and this electron flow determines the self-electric and self-magnetic fields of the beam pulse propagating through the background plasma. Furthermore, the electron potential energy in the self-electric field of the beam pulse propagating through the background plasma is large compared with the electron temperature. Therefore, the electron pressure terms can be neglected for fast ion beam pulses, in contrast to the limit of slow beams. Therefore, for the cases considered here, the electron Debye length is not relevant to the neutralization physics associated with such fast electron flow in the return current.

In this paper we have summarized a nonlinear theory describing the quasisteady-state propagation of an intense fast ion beam pulse in a background plasma, neglecting small electron thermal effects. The results of the theory have been verified by detailed comparison with particle-in-cell simulations. It has been shown that in the absence of applied magnetic field, the beam charge is well neutralized (the degree of charge neutralization is close to unity) during quasisteady-state propagation of the beam pulse through background plasma, provided that the beam pulse duration  $\tau_b$  is much longer than the electron plasma period,  $2\pi/\omega_{pe}$ , i.e.,  $\omega_{pe}\tau_b \gg 2\pi$ . Therefore, in this limit, the quasineutrality condition holds,  $n_e \approx Z_b n_b + n_p$ , where  $n_p$  is the background plasma ion density. Note, that the beam charge is well neutralized during quasisteady-state propagation of the beam pulse even through a tenuous plasma,  $n_p \ll Z_b n_b$ , after initial transient processes of neutralization during beam entry into the plasma. Tenuous plasma can provide good charge neutralization due to the accumulation of electrons from the large volume of plasma surrounding the beam pulse.<sup>28</sup> Furthermore, in the general nonlinear case with  $n_p \sim Z_b n_b$ , the

degree of current neutralization is given by Ampere's law, combined with the conservation of the generalized vorticity or canonical momentum, and the quasineutrality condition,  $n_e \approx Z_b n_b + n_p$ , i.e.,

$$B_\phi = -\frac{\partial A_z}{\partial r} = -\frac{c}{e} \frac{\partial p_{ez}}{\partial r}, \quad (51)$$

$$-\frac{1}{r} \frac{\partial}{\partial r} r \frac{\partial}{\partial r} A_z = \frac{4\pi}{c} Z_b e n_b V_{bz} - \frac{\omega_{pe}^2}{c^2} A_z. \quad (52)$$

It was shown that the ion beam current is effectively neutralized by the plasma electron current, provided the beam radius is large compared with the electron skin depth  $c/\omega_{pe}$ , i.e.,  $r_b > c/\omega_{pe}$ , and is not current neutralized in the opposite limit. This condition can be expressed as

$$I_b > 4.25(\beta_b n_b/n_p) kA, \quad (53)$$

where  $\beta_b c$  is the directed beam velocity.

Nevertheless, the degree of charge neutralization is close to unity, and the remaining self-focusing force may affect the ballistic propagation of the beam pulse over long distances. Therefore, the self-focusing force has to be considered in the design of neutralized drift compression systems. Analytical formulas have been derived for the self-focusing force taking the effects of an applied solenoidal magnetic field into account. The self-focusing force is inversely proportional to the plasma density and can be greatly reduced by increasing the plasma density. The requirement for high plasma density has been demonstrated in many numerical studies.<sup>20-22,33,59,63</sup> For ballistic propagation and focusing of intense ion beams, the degree of neutralization has to be high enough so that the remaining weak radial self-focusing force does not alter the ballistic trajectories of the beam ions. The analytical formalism that has been developed allows us to estimate the required plasma density for ballistic focusing of the beam ions.

The radial self-focusing force is strongly affected by electron inertia effects; in the absence of an applied solenoidal magnetic field, the radial self-focusing force is controlled by the electron flow in the return current,

$$F_r = m(V_b - V_{ez}) \frac{\partial V_{ez}}{\partial r}. \quad (54)$$

Here,  $V_{ez} = eA_z/mc$ , which is determined from the equation for current neutralization, Eq. (52). For the case of complete current neutralization,  $Z_b n_b V_b = n_e V_e$  and  $n_p \gg Z_b n_b$ , the radial self-focusing force is given by

$$F_r = \frac{mV_b^2 \tau_b^2}{n_p} \frac{\partial n_b}{\partial r}. \quad (55)$$

Note again that adding finite electron temperature effects yields a small correction due to the electron pressure for fast ion beam pulses, i.e.,

$$F_r = \frac{Z_b^2 (mV_b^2 - T_e)}{n_p} \frac{\partial n_b}{\partial r},$$

according to Eq. (5).

The background plasma can provide the necessary very high degree of neutralization for drift compression ( $>99\%$ ), provided the plasma density exceeds the beam density everywhere along the beam path, i.e., provided  $n_p \gg Z_b n_b$ . In the laboratory frame, the longitudinal electric field accelerates the electrons to produce the return current in the head region of the beam pulse, and decelerates electrons in the tail of the beam in order to remove the return current behind the beam pulse. The nature of this electric field is inductive, i.e., it is generated by the nonstationary self-magnetic field of the beam pulse. The radial electric field is given by

$$eE_r = -mV_{ez} \frac{\partial V_{ez}}{\partial r}. \quad (56)$$

Note that the radial electric field in the laboratory frame is positive (defocusing). The radial electric field can be described by an effective potential, which is determined from the kinetic energy of the electron flow in the return current. Thus the radial electric field is given by nonlinear terms, and can be neglected in the linear approximation.

The self-focusing force in the laboratory frame can be expressed as

$$F_r = eZ_b \left( E_r - \frac{V_b B_\phi}{c} \right), \quad (57)$$

and is dominated by the self-magnetic component of the force, i.e., the degree of charge neutralization is much higher than degree of current neutralization for long nonrelativistic beam pulses.

In the beam frame the beam propagation is typically a steady-state phenomenon. Therefore, the magnetostatic and electrostatic approximations can be used. The electric field in the beam frame is given by the potential

$$e\varphi_z^b = -m(V_b V_{ez} - V_{ez}^2/2), \quad (58)$$

and the radial self-electric field is given by

$$eE_r^b = m(V_b - V_{ez}) \frac{\partial V_{ez}}{\partial r}. \quad (59)$$

Note that the radial self-electric field in the laboratory frame is positive (defocusing), whereas the self-electric field in the beam frame is negative (focusing).

In the presence of an applied solenoidal magnetic field, the system of equations describing the self-electric and self-magnetic fields becomes much more complicated. The theory predicts that there is a sizable enhancement of the self-electric and self-magnetic fields when  $\omega_{ce} \rightarrow 2\omega_{pe}\beta_b$ . Therefore, application of a solenoidal magnetic field can be used for active control of intense ion beam transport through a background plasma.

Electromagnetic waves are generated oblique to the direction of beam propagation whenever

$$\omega_{ce} > 2\beta_b \omega_{pe}. \quad (60)$$

In the limit of a nonrelativistic beam with  $\beta_b \ll 1$ , and strong magnetic field with  $\omega_{ce} \gg 2\beta_b \omega_{pe}$ , long wavelength electromagnetic perturbations are excited with wave number  $k_{qs} \cong \beta_b \omega_{pe}^2 / \omega_{ce} c$ , and short wavelength electrostatic pertur-

bations with  $k_{qs} \cong \omega_{ce} / [\beta_b c (\omega_{ce}^2 / \omega_{pe}^2 + 1)^{1/2}]$  are also excited. The electromagnetic waves have long wavelength compared with the skin depth,

$$\lambda_{em} = \frac{cB_z}{2en_p V_b}, \quad (61)$$

whereas the short-wavelength electrostatic perturbations have short wavelength compared with the effective skin depth,

$$\lambda_{qs} = \frac{2\pi m V_b c}{eB_z} (\omega_{ce}^2 / \omega_{pe}^2 + 1)^{1/2}. \quad (62)$$

The group velocity,  $\partial\omega_{wh} / \partial k_z$  of the long-wavelength electromagnetic perturbations is larger than the beam velocity, whereas the group velocity of the short-wavelength electrostatic perturbations is smaller than the beam velocity. Therefore, the long-wavelength electromagnetic perturbations propagate ahead of the beam, whereas the short-wavelength electrostatic perturbations lag behind the beam pulse. Both wave excitations have transverse group velocity  $\partial\omega_{wh} / \partial k_x$ . Therefore, wave perturbations also propagate sideways from the beam pulse. The long-wavelength electromagnetic perturbations excited by the tail of the beam pulse can propagate along the beam and influence the dynamics of the beam head. The system reaches a quasisteady state when the wave packet of the initial transient excitation propagates sufficiently far outside the beam.<sup>63</sup> It was found, for a sufficiently long ion beam pulse, that the time scale for achieving a quasisteady state can be of order the beam pulse duration, and is therefore much longer than the inverse plasma frequency.<sup>63</sup>

The analysis in Ref. 63 determined that waves do not affect the self-focusing force in the limit of strong solenoidal magnetic field, and for beams satisfying

$$\omega_{ce} \gg 2\beta_b \omega_{pe}, \quad \text{and} \quad r_b \gg k_{qs}^{-1} = (1 + \omega_{ce}^2 / \omega_{pe}^2)^{1/2} \frac{\beta_b c}{\omega_{ce}}. \quad (63)$$

In this limit the self-magnetic field is small and does not influence the self-focusing force. Hence, the radial electric field in the beam frame is the same as the electric field in the laboratory frame and is electrostatic. The self-focusing force acting on beam ions in this case is given by

$$F_r = \frac{mV_b^2 Z_b^2}{n_p} \frac{\partial n_b}{\partial r}, \quad (64)$$

provided  $n_p \gg Z_b n_b$ .

In absence of a solenoidal magnetic field, the degrees of charge and current neutralization can be calculated by making use of Eqs. (52), (59), and (64), and the values depend on the radial profile of the beam density. An analytical estimate has been developed in Ref. 48. In the limits,  $n_b / n_p \ll 1$  and  $r_b \omega_{pe} / c \gg 1$ , it reduces to

$$\langle f \rangle = 1 - \beta_b^2 \frac{n_b}{n_p} \frac{c}{r_b \omega_{pe}}. \quad (65)$$

It can readily be shown<sup>48</sup> that the maximum deviation from quasineutrality occurs when  $r_b \sim c / \omega_{pe}$ , and the degree of

nonquasineutrality is bounded by  $(Z_b^2 Z_b n_b + n_p - n_e)/(Z_b n_b) < 0.25\beta_b^2$ . Therefore, for nonrelativistic, long ion beam pulses, there is almost complete charge neutralization. For typical heavy ion fusion parameters,  $\beta_b < 0.2$ , and the degree of charge neutralization is more than 99%.

The general expression for the effective self-electric permeance in the presence of background plasma,  $Q_{\text{eff}}$ , for arbitrary ratios of  $n_b/n_p$  and  $r_b\omega_{pe}/c$ , is also given in Ref. 48. In the limits,  $n_b/n_p \ll 1$  and  $r_b\omega_{pe}/c \gg 1$ , it reduces to

$$Q_{\text{eff}} = -\frac{Z_b m_e n_b r_b \omega_{pe}}{M n_p 2c}. \quad (66)$$

If a solenoidal magnetic field is applied with strength such that  $\omega_{ce} \gg 2\beta_b\omega_{pe}$ , and  $r_b \gg (1 + \omega_{ce}^2/\omega_{pe}^2)^{1/2}\beta_b c/\omega_{ce}$ , the radial self-electric field is negative and the ion beam space charge is overcompensated by the electrons. The average degree of charge neutralization  $\langle f \rangle$  in the limit  $Z_b n_b/n_p \ll 1$  is given approximately by

$$\langle f \rangle = 1 + 2\beta_b^2 \frac{c^2}{r_b r_g \omega_{pe}^2}. \quad (67)$$

Here,  $r_g = n_b/|(\partial n_b/\partial r)|$  is the effective radial scale of the ion beam density profile at the beam edge. Note that the second term on the right-hand side of Eq. (67) is positive because in this regime the electrons overcompensate the positive ion charge and the radial self-electric field at the beam edge is negative. The maximum deviation from quasineutrality occurs when  $r_b \cong r_g \sim \beta_b c/\omega_{pe}$ , and the beam can become non-neutralized, as observed in numerical simulations.<sup>24,25</sup> Therefore, even for nonrelativistic, long ion pulses, complete charge neutralization is not guaranteed in the presence of a solenoidal magnetic field, if  $r_b \cong r_g \sim \beta_b c/\omega_{pe}$ . However, for typical heavy ion fusion parameters,  $r_b \geq c/\omega_{pe}$  and  $\beta_b < 0.2$ , and the degree of charge neutralization can exceed more than 99% by increasing the plasma density to values satisfying  $r_b \geq c/\omega_{pe}$  according to Eq. (67).

Because the self-magnetic field contribution to the self-focusing force can be neglected in the limit  $\omega_{ce} \gg 2\beta_b\omega_{pe}$ , the total effective permeance including both self-electric and self-magnetic effects is given approximately by the self-electric permeance,

$$Q_{\text{eff}} \cong -\frac{m r_b Z_b^2 n_b}{M r_g n_p}. \quad (68)$$

In conclusion, a background plasma can provide the necessary very high degree of neutralization for drift compression of intense ion beam pulses (>99%), provided the plasma density exceeds the beam density everywhere along the beam path,  $n_p \gg Z_b n_b$ , in absence of an applied solenoidal magnetic field, and  $r_b \geq c/\omega_{pe}$ , if a solenoidal magnetic field is applied.

## ACKNOWLEDGMENTS

This research was supported by the U.S. Department of Energy under Contract No. DE-AC02-76CH-O3073 with the Princeton Plasma Physics Laboratory.

The authors are grateful to Valery Krasovitskiy, Alexey Goncharov, Scott Robertson, and Ron Cohen for fruitful discussions.

- <sup>1</sup>P. Chen, *Phys. Rev. Lett.* **54**, 693 (1985).
- <sup>2</sup>C. Joshi, *Phys. Plasmas* **14**, 055501 (2007).
- <sup>3</sup>R. Govil, W. P. Leemans, E. Yu. Backhaus, and J. S. Wurtele, *Phys. Rev. Lett.* **83**, 3202 (1999); G. Hairapetian, P. Davis, C. E. Clayton, C. Joshi, S. C. Hartman, C. Pellegrini, and T. Katsouleas, *ibid.* **72**, 2403 (1994).
- <sup>4</sup>H. Alfvén, *Phys. Rev.* **55**, 425 (1939).
- <sup>5</sup>W. H. Bennett, *Phys. Rev.* **45**, 890 (1934).
- <sup>6</sup>M. V. Medvedev, M. Fiore, R. A. Fonseca, L. O. Silva, and W. B. Mori, *Astrophys. J.* **618**, L75 (2005).
- <sup>7</sup>A. Gruzinov, *Astrophys. J.* **563**, L15 (2001); A. Spitkovsky, *ibid.* **673**, L39 (2008).
- <sup>8</sup>M. Roth, T. E. Cowan, M. H. Key, S. P. Hatchett, A. Snively, S. C. Wilks, K. Yasuike, H. Ruhl, F. Pegoraro, S. V. Bulanov, E. M. Campbell, M. D. Perry, and H. Powell, *Phys. Rev. Lett.* **86**, 436 (2001); M. Tabak, J. Hammer, M. E. Glinsky, W. L. Krueer, S. C. Wilks, J. Woodworth, E. M. Campbell, M. D. Perry, and R. J. Mason, *Phys. Plasmas* **1**, 1626 (1994); R. B. Campbell, R. Kodama, T. A. Mehlhorn, K. A. Tanaka, and D. R. Welch, *Phys. Rev. Lett.* **94**, 055001 (2005); Y. Sentoku, K. Mima, P. Kaw, and K. Nishikawa, *ibid.* **90**, 155001 (2003); T. Taguchi, T. M. Antonsen, Jr., C. S. Liu, and K. Mima, *ibid.* **86**, 5055 (2001); A. J. Kemp, Y. Sentoku, V. Sotnikov, and S. C. Wilks, *ibid.* **97**, 235001 (2006); R. J. Mason, *ibid.* **96**, 035001 (2006).
- <sup>9</sup>P. K. Roy, S. S. Yu, E. Henestroza, A. Anders, F. M. Bieniosek, J. Coleman, S. Eylon, W. G. Greenway, M. Leitner, B. G. Logan, W. L. Waldron, D. R. Welch, C. Thoma, A. B. Sefkow, E. P. Gilson, P. C. Efthimion, and R. C. Davidson, *Phys. Rev. Lett.* **95**, 234801 (2005).
- <sup>10</sup>S. S. Yu, R. P. Abbott, R. O. Bangerter, J. J. Barnard, R. J. Briggs, D. Callahan, C. M. Celata, R. Davidson, C. S. Debonnel, S. Eylon, A. Faltens, A. Friedman, D. P. Grote, P. Heitzenroeder, E. Henestroza, I. Kaganovich, J. W. Kwan, J. F. Latkowski, E. P. Lee, B. G. Logan, P. F. Peterson, D. Rose, P. K. Roy, G.-L. Sabbi, P. A. Seidl, W. M. Sharp, and D. R. Welch, *Nucl. Instrum. Methods Phys. Res. A* **544**, 294 (2005).
- <sup>11</sup>M. Reiser, *Theory and Design of Charged Particle Beams* (Wiley, New York, 1994).
- <sup>12</sup>R. C. Davidson and H. Qin, *Physics of Intense Charged Particle Beams in High Energy Accelerators* (World Scientific, Singapore, 2001).
- <sup>13</sup>M. Anderson, M. Binderbauer, V. Bystritskii, E. Garate, N. Rostoker, Y. Song, A. Van Drie, and I. Isakov, *Plasma Phys. Rep.* **31**, 809 (2005); V. Bystritskii, E. Garate, N. Rostoker, Y. Song, A. Vandrie, and M. Anderson, *J. Appl. Phys.* **96**, 1249 (2004); H. Yamada, H. Ji, S. Gerhardt, E. V. Belova, R. C. Davidson, and D. R. Mikkelsen, *J. Plasma Fusion Res.* **2**, 004 (2007); H. Ji, E. Belova, S. P. Gerhardt, and M. Yamada, *J. Fusion Energy* **26**, 93 (2007).
- <sup>14</sup>T. N. Larosa and A. Gordon, *Sol. Phys.* **120**, 343 (1989).
- <sup>15</sup>A. Gsponer, "The physics of high-intensity high-energy particle beam propagation in open air and outer-space plasmas," <http://arxiv.org/abs/physics/0409157v3>.
- <sup>16</sup>M. D. Gabovich, *Sov. Phys. Usp.* **20**, 134 (1977); I. A. Soloshenko, *Rev. Sci. Instrum.* **67**, 1646 (1996).
- <sup>17</sup>V. B. Krasovitskiy, *Sov. Phys. JETP* **32**, 98 (1971); V. B. Krasovitskiy, *Horizons in World Physics* (Nova Science, New York, 2008), Vol. 259; V. B. Krasovitskiy, *Horizons in World Physics* (Nova Science, New York, 2008), Vol. 260.
- <sup>18</sup>P. A. Seidl, A. Anders, F. M. Bieniosek, J. J. Barnard, J. Calanog, A. X. Chen, R. H. Cohen, J. E. Coleman, M. Dorf, E. P. Gilson, D. P. Grote, J. Y. Jung, M. Leitner, S. M. Lidia, B. G. Logan, P. Ni, P. K. Roy, K. Van den Bogert, W. L. Waldron, and D. R. Welch, *Nucl. Instrum. Methods Phys. Res. A* **606**, 75 (2009).
- <sup>19</sup>A. Friedman, J. J. Barnard, R. J. Briggs, R. C. Davidson, M. Dorf, D. P. Grote, E. Henestroza, E. P. Lee, M. A. Leitner, B. G. Logan, A. B. Sefkow, W. M. Sharp, W. L. Waldron, D. R. Welch, and S. S. Yu, *Nucl. Instrum. Methods Phys. Res. A* **606**, 6 (2009).
- <sup>20</sup>A. B. Sefkow, R. C. Davidson, E. P. Gilson, I. D. Kaganovich, A. Anders, J. Coleman, M. Leitner, S. M. Lidia, P. K. Roy, P. A. Seidl, P. L. Waldron, S. S. Yu, and D. R. Welch, *Phys. Plasmas* **16**, 056701 (2009); A. B. Sefkow and R. C. Davidson, *Phys. Rev. ST Accel. Beams* **10**, 100101 (2007).
- <sup>21</sup>W. M. Sharp, D. A. Callahan, M. Tabak, S. S. Yu, P. F. Peterson, D. V. Rose, and D. R. Welch *Nucl. Fusion* **44**, S221 (2004); W. M. Sharp, D. A.

- Callahan, M. Tabak, S. S. Yu, and P. F. Peterson, *Phys. Plasmas* **10**, 2457 (2003).
- <sup>22</sup>A. F. Lifschitz, G. Maynard, and J. L. Vay, *Nucl. Instrum. Methods Phys. Res. A* **544**, 202 (2005); A. F. Lifschitz, G. Maynard, J. L. Vay, and A. Lenglet, *J. Phys. IV* **133**, 753 (2006); J.-L. Vay and C. Deutsch, *Nucl. Instrum. Methods Phys. Res. A* **464**, 293 (2001); *Phys. Plasmas* **5**, 1190 (1998).
- <sup>23</sup>R. B. Miller, *An Introduction to the Physics of Intense Charged Particle Beams* (Plenum, New York, 1982).
- <sup>24</sup>I. D. Kaganovich, E. A. Startsev, A. B. Sefkow, and R. C. Davidson, *Phys. Rev. Lett.* **99**, 235002 (2007).
- <sup>25</sup>I. D. Kaganovich, E. A. Startsev, A. B. Sefkow, and R. C. Davidson, *Phys. Plasmas* **15**, 103108 (2008).
- <sup>26</sup>M. Dorf, I. D. Kaganovich, E. A. Startsev, and R. C. Davidson, *Phys. Rev. Lett.* **103**, 075003 (2009).
- <sup>27</sup>I. Kaganovich, R. C. Davidson, M. Dorf, A. B. Sefkow, E. Startsev, J. J. Barnard, A. Friedman, E. P. Lee, S. M. Lidia, B. G. Logan, P. K. Roy, P. A. Seidl, and D. R. Welch, Proceedings of 2009 Particle Accelerator Conference, Vancouver, May 2009, published online: <http://trshare.triumf.ca/~pac09proc/Proceedings/papers/th3gai03.pdf>.
- <sup>28</sup>I. D. Kaganovich, G. Shvets, E. A. Startsev, and R. C. Davidson, *Phys. Plasmas* **8**, 4180 (2001).
- <sup>29</sup>M. D. Gabovich, I. A. Soloshenko, and A. A. Ovcharenko, *Ukr. Fiz. Zh. (Russ. Ed.)* **15**, 934 (1971).
- <sup>30</sup>S. A. MacLaren, A. Faltens, P. A. Seidl, and D. V. Rose, *Phys. Plasmas* **9**, 1712 (2002).
- <sup>31</sup>C. Olson, *Proceedings of Invited Papers, The International Symposium on Heavy Ion Fusion*, Washington, DC, May 1986, edited by M. Reiser, T. Godlove, and R. Bangerter (American Institute of Physics, New York, 1986) Vol. 152, p. 215; *Nucl. Instrum. Methods Phys. Res. A* **464**, 118 (2001).
- <sup>32</sup>J. W. Poukey and S. Humphries, Jr., *Appl. Phys. (Berl.)* **33**, 122 (1978).
- <sup>33</sup>T. P. Hughes, S. S. Yu, and R. E. Clark, *Phys. Rev. ST Accel. Beams* **2**, 110401 (1999); D. R. Welch, D. V. Rose, B. V. Oliver, T. C. Genoni, R. E. Clark, C. L. Olson, and S. S. Yu, *Phys. Plasmas* **9**, 2344 (2002).
- <sup>34</sup>R. Kraft and B. R. Kusse, *J. Appl. Phys.* **61**, 2123 (1987); **61**, 2425 (1987).
- <sup>35</sup>A. Faltens and P. A. Seidl (private communication).
- <sup>36</sup>P. A. Seidl, A. Anders, F. M. Bieniosek, J. E. Coleman, J.-Y. Jung, M. Leitner, S. M. Lidia, B. G. Logan, P. N. Ni, D. Ogata, P. K. Roy, W. L. Waldron, J. J. Barnard, R. H. Cohen, D. P. Grote, M. Dorf, E. P. Gilson, and D. R. Welch, Proceedings of 2009 Particle Accelerator Conference, Vancouver, May 2009, published online: <http://trshare.triumf.ca/~pac09proc/Proceedings/papers/th3gai04.pdf>; S. M. Lidia, P. K. Roy, P. A. Seidl, W. L. Waldron, and E. P. Gilson, Proceedings of 2009 Particle Accelerator Conference, Vancouver, May 2009, published online: <http://trshare.triumf.ca/~pac09proc/Proceedings/papers/tu6pfp092.pdf>.
- <sup>37</sup>C. Burkhart and S. Humphries, Jr., Proceedings of the 12th IEEE Particle Accelerator Conference, Washington, DC, 1987 (unpublished), p. 1037.
- <sup>38</sup>Yu. M. Chekh, A. M. Dobrovolsky, A. A. Goncharov, I. M. Protsenko, and I. G. Brown, *Nucl. Instrum. Methods Phys. Res. B* **243**, 227 (2006); A. A. Goncharov and I. G. Brown, *IEEE Trans. Plasma Sci.* **35**, 986 (2007).
- <sup>39</sup>W. M. Sharp, D. A. Cahallan, and M. Tabak, *Fusion Sci. Technol.* **43**, 393 (2003); D. Callahan, *Fusion Eng. Des.* **32–33**, 441 (1996); D. R. Welch, D. V. Rose, W. M. Sharp, C. L. Olson, and S. S. Yu, *Laser Part. Beams* **20**, 621 (2002); *Nucl. Instrum. Methods Phys. Res. A* **544**, 236 (2005).
- <sup>40</sup>S. Humphries, *Charged Particles Beams* (Wiley, New York, 1990); *Appl. Phys. Lett.* **32**, 792 (1978); S. Humphries, Jr., T. R. Lockner, J. W. Poukey, and J. P. Quintenz, *Phys. Rev. Lett.* **46**, 995 (1981); R. N. Sudan, *Appl. Phys. Lett.* **44**, 957 (1984).
- <sup>41</sup>S. Humphries, Jr., *Nucl. Fusion* **20**, 1549 (1980); R. Kraft and B. Kusse, *J. Appl. Phys.* **61**, 2429 (1987).
- <sup>42</sup>I. D. Kaganovich, E. Startsev, and R. C. Davidson, *Phys. Plasmas* **11**, 3546 (2004).
- <sup>43</sup>P. K. Roy, S. S. Yu, S. Eylon, E. Henestroza, A. Anders, F. M. Bieniosek, W. G. Greenway, B. G. Logan, W. L. Waldron, D. L. Vanecek, D. R. Welch, D. V. Rose, R. C. Davidson, P. C. Efthimion, E. P. Gilson, A. B. Sefkow, and W. M. Sharp, *Phys. Plasmas* **11**, 2890 (2004); *Nucl. Instrum. Methods Phys. Res. A* **544**, 225 (2005).
- <sup>44</sup>D. A. Hammer and N. Rostoker, *Phys. Fluids* **13**, 1831 (1970); J. L. Cox and W. H. Bennett, *ibid.* **13**, 182 (1970).
- <sup>45</sup>L. S. Levine, I. M. Vitkovitsky, D. A. Hammer, and M. L. Andrews, *J. Appl. Phys.* **42**, 1863 (1971).
- <sup>46</sup>J. B. Rosenzweig, B. N. Breizman, T. Katsouleas, and J. J. Su, *Phys. Rev. A* **44**, R6189 (1991).
- <sup>47</sup>I. D. Kaganovich, A. B. Sefkow, E. A. Startsev, R. C. Davidson, and D. R. Welch, *Nucl. Instrum. Methods Phys. Res. A* **577**, 93 (2007).
- <sup>48</sup>I. D. Kaganovich, E. Startsev, and R. C. Davidson, *Laser Part. Beams* **20**, 497 (2002).
- <sup>49</sup>I. D. Kaganovich, E. Startsev, R. C. Davidson, and D. Welch, *Nucl. Instrum. Methods Phys. Res. A* **544**, 383 (2005).
- <sup>50</sup>O. Buneman, *Proc. R. Soc. London, Ser. A* **215**, 346 (1952).
- <sup>51</sup>J. D. Lawson, *Physics of Charged Particles Beams* (Clarendon, Oxford, 1988), Chap. 3.
- <sup>52</sup>H. S. Uhm and R. C. Davidson, *Phys. Fluids* **23**, 813 (1980).
- <sup>53</sup>M. N. Rosenbluth, E. P. Lee, and R. J. Briggs, "Ion pulse transport in target chamber," in *Inertial Fusion Sciences and Applications 99 (IFSA'99)*, Bordeaux, France, Sept. 12–17 (1999).
- <sup>54</sup>B. V. Oliver, P. F. Ottinger, D. V. Rose, D. D. Hinshelwood, J. M. Neri, and F. C. Young, *Phys. Plasmas* **6**, 582 (1999).
- <sup>55</sup>S. Robertson, *Phys. Rev. Lett.* **48**, 149 (1982); *Phys. Fluids* **26**, 1129 (1983); *J. Appl. Phys.* **59**, 1765 (1986).
- <sup>56</sup>R. Kraft, B. Kusse, and J. Moschella, *Phys. Fluids* **30**, 245 (1987).
- <sup>57</sup>B. V. Oliver, D. D. Ryutov, and R. N. Sudan, *Phys. Plasmas* **1**, 3383 (1994).
- <sup>58</sup>B. V. Oliver, D. D. Ryutov, and R. N. Sudan, *Phys. Plasmas* **3**, 4725 (1996).
- <sup>59</sup>A. B. Sefkow, R. C. Davidson, I. D. Kaganovich, E. P. Gilson, P. K. Roy, S. S. Yu, P. A. Seidl, D. R. Welch, D. V. Rose, and J. J. Barnard, *Nucl. Instrum. Methods Phys. Res. A* **577**, 289 (2007); Ph.D. thesis, Princeton, 2007.
- <sup>60</sup>R. N. Sudan and P. M. Lyster, *Comments Plasma Phys. Controlled Fusion* **9**, 453 (1984); D. W. Hewett, *Nucl. Fusion* **24**, 349 (1984).
- <sup>61</sup>L. D. Landau and E. M. Lifshitz, *Electrodynamics of Continuous Media* (Pergamon, Oxford, New York, 1993).
- <sup>62</sup>C. M. Celata, F. M. Bieniosek, E. Henestroza, J. W. Kwan, E. P. Lee, G. Logan, L. Prost, P. A. Seidl, J. L. Vay, W. L. Waldron, S. S. Yu, J. J. Barnard, D. A. Callahan, R. H. Cohen, A. Friedman, D. P. Grote, S. M. Lund, A. Molvik, W. M. Sharp, G. Westenskow, R. C. Davidson, P. Efthimion, E. Gilson, L. R. Grisham, I. Kaganovich, H. Qin, E. A. Startsev, S. Bernal, Y. Cui, D. Feldman, T. F. Godlove, I. Haber, J. Harris, R. A. Kishek, H. Li, P. G. O'Shea, B. Quinn, M. Reiser, A. Valfells, M. Walter, Y. Zou, D. V. Rose, and D. R. Welch, *Phys. Plasmas* **10**, 2064 (2003); B. G. Logan, F. M. Bieniosek, C. M. Celata, E. Henestroza, J. W. Kwan, E. P. Lee, M. Leitner, P. K. Roy, P. A. Seidl, S. Eylon, J.-L. Vay, W. L. Waldron, S. S. Yu, J. J. Barnard, D. A. Callahan, R. H. Cohen, A. Friedman, D. P. Grote, M. Kireeff Covo, W. R. Meier, A. W. Molvik, S. M. Lund, R. C. Davidson, P. C. Efthimion, E. P. Gislou, L. R. Grisham, I. D. Kaganovich, H. Qin, E. A. Startsev, D. V. Rose, D. R. Welch, C. L. Olson, R. A. Kishek, P. O'Shea, I. Haber, and L. R. Prost, *Nucl. Instrum. Methods Phys. Res. A* **577**, 1 (2007).
- <sup>63</sup>M. A. Dorf, I. D. Kaganovich, E. A. Startsev, and R. C. Davidson, *Phys. Plasmas* **17**, 023103 (2010).
- <sup>64</sup>A. I. Ahiezer, I. A. Ahiezer, R. V. Polovin, A. G. Sitenko, and K. N. Stepanov, *Plasma Electrodynamics* (Nauka, Moscow, 1974).
- <sup>65</sup>J. Lavergnat and R. Pellat, *J. Geophys. Res.* **84**, 7223, doi:10.1029/JA084iA12p07223 (1979).
- <sup>66</sup>C. Krafft, P. Thévenet, G. Matthieussent, B. Lundin, G. Belmont, B. Lembège, J. Solomon, J. Lavergnat, and T. Lehner, *Phys. Rev. Lett.* **72**, 649 (1994).
- <sup>67</sup>A. Volokitin, C. Krafft, and G. Matthieussent, *Phys. Plasmas* **2**, 4297 (1995).
- <sup>68</sup>A. Volokitin, C. Krafft, and G. Matthieussent, *Phys. Plasmas* **4**, 4126 (1997).
- <sup>69</sup>C. Krafft and A. Volokitin, *Phys. Plasmas* **5**, 4243 (1998).
- <sup>70</sup>N. Brenning, T. Hurtig, and M. A. Raadu, *Phys. Plasmas* **12**, 012309 (2005); T. Hurtig, N. Brenning, and M. A. Raadu, *ibid.* **10**, 4291 (2003).